

This discussion paper is/has been under review for the journal *Climate of the Past* (CP).
Please refer to the corresponding final paper in CP if available.

Effects of melting ice sheets and orbital forcing on the early Holocene warming in extratropical Northern Hemisphere

Y. Zhang^{1,2}, H. Renssen², and H. Seppä¹

¹Department of Geosciences and Geography, University of Helsinki, P.O. Box 64, FI00014 Helsinki, Finland

²Faculty of Earth and life Sciences, VU University Amsterdam, De Boelelaan 1085, 1081 HV Amsterdam, the Netherlands

Received: 13 October 2015 – Accepted: 29 October 2015 – Published: 12 November 2015

Correspondence to: Y. Zhang (yurui.zhang@helsinki.fi)

Published by Copernicus Publications on behalf of the European Geosciences Union.

CPD

11, 5345–5399, 2015

Effects of melting ice sheets and orbital forcing

Y. Zhang et al.

Title Page

Abstract

Introduction

Conclusions

References

Tables

Figures



Back

Close

Full Screen / Esc

Printer-friendly Version

Interactive Discussion



Abstract

The early Holocene is a critical period for climate change, as it marked the final transition from the last deglaciation to the relatively warm and stable Holocene. It is characterized by a warming trend that has been registered in numerous proxy records. This climatic warming was accompanied by major adjustments in different climate components, including the decaying of ice sheets in cryosphere, the perturbation of circulation in the ocean, the expansion of vegetation (over the high latitude) in biosphere. Previous studies have analyzed the influence of the demise of the ice sheets and other forcings on climate system. However, the climate response to the forcings together with the internal feedbacks before 9 ka remains not fully comprehended. In this study, we therefore disentangle how these forcings contributed to climate change during the earliest part of Holocene (11.5–7 ka) by employing the LOVECLIM climate model for both equilibrium and transient experiments.

The results of our equilibrium experiments for 11.5 ka reveal that the annual mean temperature at the onset of the Holocene was lower than in the preindustrial era in the Northern extratropics, except in Alaska. The magnitude of this cool anomaly varies regionally as a response to varying climate forcings and diverse mechanisms. In eastern N America and NW Europe the temperatures throughout the whole year were 2–5 °C lower than in the preindustrial control, reaching the maximum cooling as here the climate was strongly influenced by the cooling effects of the ice sheets. This cooling of the ice-sheet surface was caused both by the enhanced surface albedo and by the orography of the ice sheets. For Siberia, a small deviation (–0.5–1.5 °C) in summer temperature and 0.5–1.5 °C cooler annual climate compared to the preindustrial run were caused by the counteraction of the high albedo associated with the tundra vegetation which was more southward extended at 11.5 ka than in the preindustrial period and the orbitally induced radiation anomalies. In the eastern part of the Arctic Ocean (over Barents Sea, Kara Sea and Laptev Sea), the annual mean temperature was 0.5–2 °C lower than at 0 ka, because the cooling effect of a reduced northward heat transport

CPD

11, 5345–5399, 2015

Effects of melting ice sheets and orbital forcing

Y. Zhang et al.

Title Page

Abstract

Introduction

Conclusions

References

Tables

Figures



Back

Close

Full Screen / Esc

Printer-friendly Version

Interactive Discussion



Effects of melting ice sheets and orbital forcing

Y. Zhang et al.

Title Page

Abstract

Introduction

Conclusions

References

Tables

Figures



Back

Close

Full Screen / Esc

Printer-friendly Version

Interactive Discussion



induced by the weakened ocean circulation overwhelmed the orbitally induced warming. The 0.5–3 °C cooler climate over the N Labrador Sea and N Atlantic Ocean was related to the reduced northward heat transport and sea-ice feedbacks initiated by the weakened ocean circulation. In contrast, in Alaska, temperatures in all seasons were 0.5–3 °C higher than the control run primarily due to the orbitally induced positive insolation anomaly and also to the enhanced southerly winds which advected warm air from the South as a response to the high air pressure over the Laurentide Ice Sheet.

Our transient experiments indicate that the Holocene temperature evolution and the early Holocene warming also vary between different regions. In Alaska, the climate is constantly cooling over the whole Holocene, primarily following the decreasing insolation. In contrast, in N Canada, the overall warming during the early Holocene is faster than in other areas (up to 1.88 °C ka⁻¹ in summer) as a consequence of the progressive decay of the LIS, and the warming lasted till about 7 ka when this deglaciation was completed. In NW Europe, the Arctic and Siberia, the overall warming rates are intermediate with about 0.3–0.7 °C ka⁻¹ in most of seasons (with only exception in Arctic's winter). Overall, our results demonstrate the spatial variability of the climate during the early Holocene, both in terms of the temperature distribution and warming rates, as the response to varying dominant forcings and diverse mechanisms.

1 Introduction

The early Holocene is palaeoclimatologically interesting as it represents the last transition phase from full glacial to interglacial conditions. Oxygen isotope measurements from ice cores in Greenland (Dansgaard et al., 1993; GRIP Members, 1993; Grootes et al., 1993; Rasmussen et al., 2006; Vinther et al., 2006, 2008) and the Canadian high-Arctic (Koerner and Fisher, 1990) consistently reflect a shift in $\delta^{18}\text{O}$ stable-isotope by up to 3–5‰ during the early Holocene and then stay at a relatively stable level. This isotopic shift implies changes in the climate system, for instance a couple of degrees warming from 11.5 to 7 ka BP (hereafter noted as ka) (Dahl-Jensen et al., 1998; Vinther

Effects of melting ice sheets and orbital forcing

Y. Zhang et al.

Title Page

Abstract

Introduction

Conclusions

References

Tables

Figures



Back

Close

Full Screen / Esc

Printer-friendly Version

Interactive Discussion



et al., 2009). This early-Holocene warming trend is also registered in biological proxies, for example a 4–5°C warming in western and northern Europe indicated by chironomids, plant macrofossils and pollen assemblages from lake sediments (Brooks and Birks, 2000; Brooks et al., 2012; Birks, 2015). In addition, this transition is recorded in many other high-resolution records further East in Eurasia, for example in speleothems from China (Yuan et al., 2004; Wang et al., 2005). Apart from these land-based observations, comparable trends are identified in marine sediment core data, such as a rise in sea surface temperature during the early Holocene in the N Atlantic reflected by the variation in $\delta^{18}\text{O}$ values and in abundance of planktonic foraminifera (Bond et al., 1993; Kandiano et al., 2004; Hald et al., 2007). Overall, proxy temperature stacks reveal a 3°C warming in Northern Hemisphere in the early Holocene (Shakun et al., 2012). Although these proxy records provide a general view of early Holocene warming, its detailed expression in different regions and the reasons for spatial variations are poorly known.

It is well accepted that the orbitally induced increase in Northern Hemisphere summer insolation was the main external driver of the climate change during the last deglaciation (Berger, 1988; Denton et al., 2010; Abe-Ouchi et al., 2013; Buizert et al., 2014). This increase peaked in the earliest Holocene at 11 ka. For instance, at 60° N June insolation at 11 ka was 47 W m^{-2} above the present-day value (Berger, 1978). In addition to this external orbital forcing, the early Holocene was characterized by critical adjustments in climate components (e.g., in cryosphere, ocean and biosphere) that further affected the temperature through various feedbacks. In the cryosphere, the Laurentide ice Sheet (LIS) and Fennoscandian Ice Sheet (FIS) were melting at a fast rate and eventually demised around 6.8 and 10 ka, respectively (Dyke et al., 2003; Occhietti et al., 2011), which exerted multiple influences on the climate system (Renssen et al., 2009). For instance, several studies have found that the global ocean circulation is sensitive to freshwater fluxes generated from the melting ice sheets in terms of varying locations related to deep convection and flow rates (Renssen et al., 2010; Roche et al., 2010). Indeed, proxy-based evidence suggested that ice sheet melting in the

Effects of melting ice sheets and orbital forcing

Y. Zhang et al.

[Title Page](#)

[Abstract](#)

[Introduction](#)

[Conclusions](#)

[References](#)

[Tables](#)

[Figures](#)



[Back](#)

[Close](#)

[Full Screen / Esc](#)

[Printer-friendly Version](#)

[Interactive Discussion](#)



early Holocene and the resulting freshening of the surface ocean slowed down the Atlantic Meridional Overturning Circulation (AMOC), leading to reduced northward heat transport, and then cold conditions and extended sea ice cover over mid and high latitudes (Thornalley et al., 2009, 2011, 2013). In addition, compared to ice-free surfaces, the surface albedo was much higher over the ice sheets, also resulting in relatively low temperature. Furthermore, the topography of ice sheets also can influence the climate through adjustment of the atmospheric circulation which can vary from region to region (Felzer et al., 1996; Justino and Peltier, 2005; Langen and Vinther, 2009). For instance, topography of ice sheets generated the glacial anticyclone that locally cooled the temperature (Felzer et al., 1996). In contrast, the topography effects of ice sheet caused a 2–3 °C warming over the North Atlantic under the Last Glacial Maximum (LGM) context (Pausata et al., 2011; Hofer et al., 2012). However, the net effect of ice sheet on climate caused a cooling in the mid and high latitudes when all of these ice sheet related aspects – orography, extent and the meltwater – are taken into account. For the early Holocene, although the ice sheets were substantially reduced in scale compared to the LGM, the net cooling effect of the ice sheets still can be seen, and they tempered the impact of the orbitally forced summer insolation maximum (Renssen et al., 2009). The regional differences caused by the impact of ice sheets relative to insolation were reflected by the clear regional variations in timing of the Holocene thermal maximum (HTM) among similar latitudes. For instance, Alaska had a much earlier HTM than eastern Canada (Kaufman et al., 2004). However, the main sources of uncertainty on early Holocene climate change are associated with the dynamics of ice sheets and the related freshwater release. For example, deglaciation reconstructions are primarily based on dating of geological features and correlating these geological datasets between regions (Dyke et al., 2003; Svendsen et al., 2004; Putkinen and Lunkka, 2008; Stokes et al., 2015). Recent studies based on cosmogenic exposure dating indicate slightly older ages of deglaciation in some regions than suggested by radiocarbon dating (Carlson et al., 2014; Clark, 2015), because a large uncertainty in bulk organic sample's ages and the possibility of old carbon contamination (Carlson et al., 2014;

et al., 2003; Occhietti et al., 2011; Clark, 2015). Moreover, the Younger Dryas stadial ended at 11.7 ka and may still have influenced the early Holocene climate due to the long response time of the deep ocean (Renssen et al., 2012). Therefore, before 9 ka the climate system's response to forcings, especially to ice sheets, is poorly comprehended.

Here, we extend the study of Blaschek and Renssen (2013) back to 11.5 ka for exploring the early-Holocene climate response to these key forcings in the northern extratropics. We employ the same climate model of intermediate complexity LOVECLIM that includes dynamical components for the atmosphere, ocean, sea ice and vegetation. We first analyze the impact of forcings on the climate at 11.5 ka in equilibrium experiments and subsequently investigate the influence of two ice-sheet deglaciation scenarios in transient simulations. By comparing the simulations we try to disentangle how the dynamic ice sheets influenced the early-Holocene climate and the possible mechanisms. More specifically, we address the following research questions: (1) What are the main spatial characteristics of temperature at the onset of Holocene (11.5 ka)? (2) What is the role of forcings, especially ice sheet decay, in shaping these characteristics and what are possible other mechanisms? (3) What are the overall features of the temperature evolution and the early Holocene warming in different regions?

2 Model and experimental design

2.1 The LOVECLIM model

We conducted our simulations with version 1.2 of the three-dimensional Earth system model of intermediate complexity LOVECLIM (Goosse et al., 2010), in which the components of the atmosphere, ocean and sea ice, vegetation, ice sheets and carbon cycle are dynamically included. However, in our version, the components for ice sheets and the carbon cycle were not activated. Accordingly, the ice sheet configuration was prescribed. The atmospheric component is the quasi-geostrophic model ECBilt cou-

Effects of melting ice sheets and orbital forcing

Y. Zhang et al.

Title Page

Abstract

Introduction

Conclusions

References

Tables

Figures



Back

Close

Full Screen / Esc

Printer-friendly Version

Interactive Discussion



Effects of melting ice sheets and orbital forcing

Y. Zhang et al.

Title Page

Abstract

Introduction

Conclusions

References

Tables

Figures



Back

Close

Full Screen / Esc

Printer-friendly Version

Interactive Discussion



pled to a land-surface model. It consists of 3 vertical layers and has T_{21} horizontal resolution (Opsteegh et al., 1998). CLIO is the ocean component which consists of a free-surface, primitive-equation oceanic general circulation model (GCM) coupled to a three-layer dynamic-thermodynamic sea-ice model (Fichefet and Maqueda, 1997).

The ocean model includes 20 vertical levels and a $3^\circ \times 3^\circ$ latitude–longitude horizontal resolution (Goosse and Fichefet, 1999). These two core components were further coupled to the biosphere model VECODE, which simulates the dynamics of two main terrestrial plant functional types, trees and grasses, as well as desert (Brovkin et al., 1997). More details on LOVECLIM can be found in Goosse et al. (2010).

LOVECLIM is a useful tool to explore the mechanisms behind climate change and has made critical contributions to our understanding of Holocene long-term climate change observed in proxy records (Renssen et al., 2005, 2006, 2010). For example, experiments with realistic freshwater perturbations for the 8.2 ka event reproduced a climate anomaly that compared favorably with proxy data both with respect to magnitude of the cooling and the duration of the events (Renssen et al., 2002; Wiersma et al., 2006). Transient experiments of the last 9 ka have revealed that the decaying LIS delayed the timing of HTM in terms of temperature evolution (Renssen et al., 2009) and that the climate was sensitive to GIS melting (Blaschek and Renssen, 2013) during the Holocene. The LOVECLIM model simulates a reasonable modern climate, as the simulation set up with present-day forcing is able to capture the main characteristics of the observed temperature distribution in the extratropics (Goosse et al., 2010), although the model seems to overestimate the temperature over the tropics and produces a weaker temperature gradient between the Eastern and Western Pacific Ocean than observed. Moreover, the model also simulates meridional overturning streamfunction which agrees with the data-based estimates and other models, even though the simulated sea ice extent is better in the Pacific than in the Atlantic. It also reproduces a large-scale structure of atmosphere circulation which is comparable with observations, except for a slightly weaker Aleutian low and a location shift of the Icelandic low (Goosse et al., 2010). In addition, the model's sensitivity to freshwater perturbation

is reasonable (Roche et al., 2007), and to a doubling of atmospheric CO₂ concentration is 2K, which is in the lower range of coupled general circulation models (GCMs) (Martinez-Boti et al., 2015; Palaeosens Members, 2015).

2.2 Prescribed forcings

We included the major climatic forcings in terms of greenhouse gas concentrations in the atmosphere, astronomical parameters (orbital forcing) and decaying ice sheets. In all simulations, the solar constant, aerosol levels, the continental configuration and bathymetry were kept fixed at preindustrial values. Considering the greenhouse gas (GHG) forcing, we based the concentrations of CO₂, CH₄ and N₂O on measurements in ice cores (Loulergue et al., 2008; Schilt et al., 2010). From the onset of the Holocene, the radiative GHG forcing anomaly (relative to 0 ka) in W m⁻², representing the overall GHG contribution, showed first a rapid rise with a peak of -0.3 W m⁻² at 10 ka, followed by a slight decrease towards a minimum at 7 ka, and gradual increase towards 0 ka (Fig. 1). For the orbital configuration (ORB), the values of the astronomical parameters, eccentricity, obliquity and longitude of perihelion, which determine the latitudinal and seasonal distribution of solar radiation at the top of atmosphere, were derived from Berger (1978). As an example of the resulting change in insolation, the anomaly for June at 65° N is plotted in Fig. 1, showing the gradual decrease over the course of the Holocene. At the beginning of Holocene (11.5 ka), the orbitally-induced insolation anomaly in Northern Hemisphere (NH) was positive in summer and negative in winter (Fig. 2). At the same time, the global annual-mean insolation stayed almost at the same level (not shown). Therefore, the obliquity is most likely the major contributing factor for the orbital forcing in this case. Overall, this setup of GHG and ORB forcing is in line with the PMIP3 protocol (<https://pmip3.lsce.ipsl.fr/>), except for the increases in GHG levels in the industrial era, which were excluded (Ruddiman, 2007).

For the ice sheet forcing, we took three aspects into account – their spatial extent, thickness and meltwater discharge. The reconstructions of ice-sheet extent and deglaciation are primarily based on the dating of geological features, such as former

Effects of melting ice sheets and orbital forcing

Y. Zhang et al.

Title Page

Abstract

Introduction

Conclusions

References

Tables

Figures



Back

Close

Full Screen / Esc

Printer-friendly Version

Interactive Discussion



end moraines and glaciated terrain, and on correlation of these geological datasets between different regions. According to the reconstructions, at 11.5 ka the ice sheets covered most of Fennoscandia except for southern Scandinavia and eastern Finland (Svendsen et al., 2004; Putkinen and Lunkka, 2008; Clark, 2015). The LIS occupied most of the lowland area north of the Great Lakes region and filled the whole Hudson Strait (Licciardi et al., 1999; Dyke et al., 2003; Occhietti et al., 2011). According to Ganopolski et al. (2010), the relative thickness of LIS was up to 2000 m, while for the FIS this was about 100 m. Both the spatial extent of ice sheet and the maximum thickness decreased rapidly during the earliest Holocene, followed by a more gradual deglaciation rate from 8 ka onward (Fig. 3a).

In our equilibrium experiments for 11.5 ka, we applied the meltwater release for 1200 yrs by adding 0.11 Sv (Sverdrup: $10^6 \text{ m}^3 \text{ s}^{-1}$) of freshwater at the St. Lawrence River and 0.05 Sv at Hudson Strait and Hudson River, 0.055 Sv from FIS and 0.002 Sv from GIS (Licciardi et al., 1999; Jennings et al., 2015). In our transient experiments that covered the last 11.5 ka, the total freshwater volume added into oceans due to ice sheet melting is about $1.46 \times 10^{16} \text{ m}^3$ in the first 4700 yrs, which roughly matches with the estimated volume of ice sheet melted in the early Holocene (Dyke et al., 2003; Ganopolski et al., 2010; Clark, 2015). The volume of meltwater is slightly lower than the volume of the estimated 60 m sea level rise during the early Holocene (Lambeck et al., 2014), thus suggesting a coeval Antarctic melting contribution that is not considered here. Given the lack of climate imprint and hence the relatively large uncertainty in freshwater forcing, we used two versions of the freshwater flux (Fig. 3b) that represent two possible deglaciation scenarios of the GIS and FIS, named FWF-v1 and FWF-v2. Compared to FWF-v1, the second version of freshwater flux included a larger GIS contribution in the earliest Holocene (before 9 ka) in agreement with Vinther et al. (2009), and a more gradually decreasing melting rate of the FIS. However, the freshwater discharge from LIS stayed the same as in version-1, since the LIS deglaciation has been relatively well studied and we are more certain about its contribution.

CPD

11, 5345–5399, 2015

Effects of melting ice sheets and orbital forcing

Y. Zhang et al.

Title Page

Abstract

Introduction

Conclusions

References

Tables

Figures



Back

Close

Full Screen / Esc

Printer-friendly Version

Interactive Discussion



2.3 Setup of experiments

We performed two types of experiments: equilibrium and transient simulations. Firstly, a series of equilibrium experiments with boundary conditions for 11.5 ka (Table 1) were designed, of which only two simulations are presented here: OG11.5 with only ORB and GHG forcings, and OGIS11.5 with full forcing (including the ice sheets). Each of these was run for 1200 yrs from the model's default modern condition to spin-up and the last 200 yrs data were used for the analysis, as Renssen et al. (2006) demonstrated that such a spin-up is sufficient to produce a realistic climate.

The end of the 1200 yrs equilibrium runs was then taken to obtain realistic initial conditions for three transient experiments that covered the last 11.5 ka. In the first transient simulation named ORBGHG, GHG and ORB vary on an annual basis. In the second simulation OGIS_FWF-v1, the ice sheet forcing in terms of the ice extent and elevation (Fig. 3a) was included in addition to GHG and ORB, and the version-1 of freshwater flux (Fig. 3b) was applied. A comparison between ORBGHG and OGIS_FWF-v1 allows us to explore the influence of ice sheets. In order to further investigate the sensitivity of climate to the relatively uncertain freshwater forcing related to the melting of GIS and FIS, a third experiment (named OGIS_FWF-v2) was performed with version-2 freshwater (Fig. 3c), while the topography of all ice sheets was kept the same as in OGIS_FWF-v1. A pre-industrial experiment (PI) was run for 1200 yrs from the model's default modern condition with the boundary conditions in Table 1 and, similarly as for the other equilibriums, the results of the last 200 yrs were used as a reference. All temperature values in this study are shown as deviations from this reference.

3 Results

In the first part of this section, our analysis and discussion of temperatures is based on equilibrium experiments, which are designed to study the response of the climate to the main forcings at 11.5 ka and to obtain the realistic 11.5 ka climate state. Then, in

CPD

11, 5345–5399, 2015

Effects of melting ice sheets and orbital forcing

Y. Zhang et al.

Title Page

Abstract

Introduction

Conclusions

References

Tables

Figures



Back

Close

Full Screen / Esc

Printer-friendly Version

Interactive Discussion



the second part, based on the analysis of the first part, we mainly focus on the transient simulations for tracing the temperature evolution during the last 11.5 ka.

3.1 Equilibrium experiments at the onset of the Holocene

3.1.1 Simulation with only ORB and GHG forcings at 11.5 ka (OG11.5)

5 In experiment OG11.5, summer temperatures are 2–4 °C higher over most of extratropical continents than in our preindustrial reference run, with the maximum difference of 5 °C in the central part of continents (Fig. 4a). The warming over the oceans is less conspicuous with a 1.5 °C warmer climate, indicating lower sensitivity of oceans to the prescribed forcings than continents. As all atmospheric greenhouse gas levels were
10 lower at 11.5 ka than in preindustrial era (Fig. 1), the warmer conditions in OG11.5 are caused by the orbitally-induced positive summer insolation anomaly.

The most obvious feature of the simulated winter temperature anomaly is the marked contrast between high latitudes and areas more to the South (Fig. 4b). For instance, the mid-latitudes are 1.5–3 °C cooler than in the reference run PI with the strongest
15 cooling in the central part of continents, while the Arctic is clearly warmer with a maximum up to +3 °C. With the exception of the Arctic, the OG11.5 results clearly reflect a stronger seasonality than present day with warmer summer and cooler winter, which is consistent with the insolation change at 11.5 ka (Fig. 2). Annual temperatures are about 1–4 °C higher at the high latitudes compared to the PI, whereas in temperate
20 regions the temperatures are roughly unchanged (mostly within 0.5 °C, Fig. 4c).

3.1.2 Climate response to melting ice sheets at 11.5 ka (OGIS11.5)

As expected, our simulation OGIS11.5 including the impact of 11.5 ka ice sheets suggests a much cooler climate than in the OG11.5 ka experiment. Most notably, ice sheets change the summer temperature pattern by inducing a strong cooling over ice-covered
25 areas, reducing temperatures by 5 °C compared to our reference run, with maximum

Effects of melting ice sheets and orbital forcing

Y. Zhang et al.

Title Page

Abstract

Introduction

Conclusions

References

Tables

Figures



Back

Close

Full Screen / Esc

Printer-friendly Version

Interactive Discussion



cooling at the center of the LIS and FIS. Additionally, the sea surface temperature is also more than 1.5°C lower over N Atlantic Ocean. In contrast, summer temperatures are mostly above the preindustrial level over the ice-free continents, but still lower than in OG11.5, except for NW Canada and Alaska.

5 Despite the impact of the ice sheets in OGIS11.5, the central Arctic remains warmer in winter than in the preindustrial era, similar to the results of OG11.5. On the other hand, the area with colder conditions clearly expands in OGIS11.5 compared to OG11.5, with anomalies reaching well below -5°C. Alaska is the only continental region where the winter temperatures are above the preindustrial mean by up to +3°C. As
10 expected, the maximum cooling effect is present in the regions covered by ice sheets, for instance more than 3°C over the LIS.

In OGIS11.5, the simulated annual mean temperature anomalies clearly show that the overall climate is cooler than in the PI due to the impact of the ice sheets. The Eurasian continent is mostly 1.5–3°C cooler, and a maximum temperature reduction
15 of more than 5°C is simulated over the LIS and FIS. Only two areas are still warmer: Alaska, including the adjacent sector of the Arctic Ocean, and the Nordic Seas. The most distinct feature in OGIS11.5 is thus a thermally contrasting pattern over North America, with simulated temperatures being around 2°C higher than the preindustrial reference in Alaska, while in most of Canada the temperatures are more than 3°C
20 lower.

3.2 Transient simulation for the Holocene

To further investigate the potential impact of ice sheets on the temperature trend we now analyze the transient simulations. In our analysis in Sect. 3.1, it became clear that the climate shows different responses in the following areas: the Arctic, NW Europe,
25 N Canada, Alaska and Siberia (marked in Fig. S1 in the Supplement). Therefore, these areas are selected for special examination and the temperature evolutions of these regions will be shown. Since our major focus is on the millennial-scale tempera-

Effects of melting ice sheets and orbital forcing

Y. Zhang et al.

Title Page

Abstract

Introduction

Conclusions

References

Tables

Figures



Back

Close

Full Screen / Esc

Printer-friendly Version

Interactive Discussion



ture trends, we applied a 500 yr running mean to our simulated time-series, effectively filtering out high-frequency variability.

3.2.1 Temperature evolution in the Arctic

In the simulation ORBGHG, the summer temperature in the Arctic continuously decreases, resulting in a total cooling of 2 °C during the Holocene. The winter temperature shows an overall cooling that is even stronger, reaching about 3 °C, even though temperature slightly increases at the very beginning. The simulated annual mean temperature displays a cooling that is intermediate between that of the summer and winter seasons (Fig. 5).

Compared to ORBGHG, the simulation OGIS_FWF-v1 with full forcings reveals a more complicated climate evolution. At the onset of Holocene, the effect of ice sheets causes the temperature in both summer and winter to be more than 2 °C lower than in ORBGHG. It is no surprise that the simulated effect of the ice sheets is larger at the beginning of the Holocene than afterwards when the deglaciation has progressed further. The final deglaciation of FIS happens at 10 ka and LIS at 6.8 ka (Fig. 3a) and thus their cooling effects no longer exist after 6.5 ka, and therefore all three runs show similar temperatures after that time. As a consequence, the temperature evolution curve of OGIS_FWF-v1 first shows a warming, with the peak reached when the cooling effects of the ice sheets are counterbalanced by the insolation, followed by a gradual cooling that is controlled by the orbital forcing. The temperature initially increases till around 6.5 ka at rate of about 0.35, 0.28 and 0.51 °Cka⁻¹ for summer, winter and annual temperature, respectively. The simulation OGIS_FWF-v1 indicates that the summer climate in Arctic experiences a slightly faster warming at the beginning, followed by a more gradual warming till the maximum anomaly of 1 °C warmer than present day at about 7.5 ka (Fig. 5a). The simulated winter temperature stays at a lower level, being 2 °C lower than in ORBGHG till 7 ka, followed by a rapid increase of about 1.5 °C within 500 yrs, reaching a warm maximum of about 1.5 °C warmer than today. The simulated annual mean temperatures show a relatively stable rise till 6.5 ka reaching a maxi-

Effects of melting ice sheets and orbital forcing

Y. Zhang et al.

Title Page

Abstract

Introduction

Conclusions

References

Tables

Figures



Back

Close

Full Screen / Esc

Printer-friendly Version

Interactive Discussion



imum of about 1.5 °C warmer than the reference. The simulation OGIS_FWF-v2 gives rather similar results in the Arctic, but has an even cooler climate before 9 ka than in OGIS_FWF-v1 with the maximum cooling up to 0.3 °C in all seasons at 10.5 ka.

3.2.2 Temperature evolution in Northwestern Europe

5 In the domain of Northwestern Europe, ORBGHG indicates smaller climate variability during all seasons than in the Arctic. The temperature declines by around 1.5 °C over the entire period in summer, less than 0.5 °C in annual mean and rises by 0.5 °C in winter (Fig. 6). This contrasts markedly with the clear cooling of climate in each season in the Arctic, and implies a stronger seasonality than in the preindustrial period.

10 The simulation OGIS_FWF-v1 shows an overall cooler climate in NW Europe at the onset of Holocene than at 0 ka, with the temperature anomalies of -1.5 °C in summer, -3 °C in winter and -2.8 °C in annual mean compared to the pre-industrial era. From that time on, the temperatures increase in the early Holocene at an overall rate of 0.73, 0.51 and 0.55 °C ka⁻¹ for summer, winter and annual mean, respectively. The most
15 important feature in summer is a sharp rise of temperature from a negative anomaly (-1.5 °C) to a positive one (+1 °C) by 10 ka, when a first peak is reached. Subsequently, a slight cooling is noted till 8 ka, followed by another temperature increase which leads to a second warming peak at 7.4 ka. In winter, the climate shows a relatively stable warming till 6.5 ka with no identifiable warm peak. The annual temperature reflects the
20 same phases of warming as in summer, one before 10 ka and another before 7.5 ka, but without a clear early temperature maximum. From around 7 ka, the temperatures in all seasons follow the ORBGHG simulation. It is worth noticing that the simulation OGIS_FWF-v2 produces a further cooler climate in summer between 11.5 and 9 ka than OGIS_FWF-v1, which is also reflected in the annual mean. As a result, there is
25 only one clear thermal maximum in summer, peaking at about 7.4 ka.

Effects of melting ice sheets and orbital forcing

Y. Zhang et al.

Title Page

Abstract

Introduction

Conclusions

References

Tables

Figures



Back

Close

Full Screen / Esc

Printer-friendly Version

Interactive Discussion



3.2.3 Temperature evolution in Northern Canada

In ORBGHG, simulated temperatures in N Canada decrease by 2.2°C in summer, 0.6°C in winter and 1.1°C in annual average during the Holocene (Fig. 7). The stronger cooling in summer than in winter reflects the strong early-Holocene seasonality which decreases over the whole period.

The simulation OGIS_FWF-v1 produces a much cooler climate in N Canada during the early Holocene than in ORBGHG. Compared to ORBGHG, the climate is cooler at the onset of Holocene by more than 5°C in all seasons. As expected, the climate in N Canada is dramatically warming up with an overall large rate varying from 1.37°Cka⁻¹ in winter to 1.88°Cka⁻¹ in summer in the early Holocene owing to the impact of gradually decaying LIS. The early Holocene warming is however not linear, as an initial phase with more rapid warming is followed by a more gradual temperature increase. In summer the warming results in a thermal maximum at around 7.4 ka that is about 1°C warmer than at preindustrial period. From that time on, the climate experiences a gradual cooling that is very similar to the ORBGHG. Compared to summer, the simulated temperatures in winter and annual mean do not show such a clear thermal maximum. The results of OGIS_FWF-v2 only indicate marginal differences relative to OGIS_FWF-v1 in all seasons. Overall, the most significant feature in the simulated temperature evolution in N Canada is the impressive warming in the early Holocene.

3.2.4 Temperature evolution in Alaska

In Alaska, the ORBGHG simulation represents an overall cooling trend for all seasons. The simulated summer and annual mean temperatures experience a decrease by more than 2°C over the whole period. The winter temperature slightly increases till about 10 ka and then stays about 2°C higher than in the PI for about 800 yrs, followed by a constant decrease to the preindustrial reference.

In contrast to other areas, both summer and winter temperatures in OGIS_FWF-v1 show an overall cooling trend in Alaska during the entire Holocene (Fig. 8), which is

Effects of melting ice sheets and orbital forcing

Y. Zhang et al.

Title Page

Abstract

Introduction

Conclusions

References

Tables

Figures



Back

Close

Full Screen / Esc

Printer-friendly Version

Interactive Discussion



rather similar to our ORBGHG simulation, although the early Holocene is even slightly warmer in OGIS_FWF-v1. As in ORBGHG, the simulation OGIS_FWF-v1 indicates a 2°C decline in summer temperature over the whole period, although a slightly faster rate than in ORBGHG can be seen between 7 and 6.5 ka. The simulated winter temperature is clearly higher than in ORBGHG at 11.5 ka, and decreases by 3.5°C over the early Holocene, with two small drops at 9.5 and 6.7 ka. The annual temperature in OGIS_FWF-v1 reflects a 2.3°C cooling during the Holocene. The OGIS_FWF-v2 shows slightly cooler climate before 9 ka than OGIS_FWF-v1, especially in winter.

3.2.5 Temperature evolution in Siberia

In Siberia, summer temperature in ORBGHG declines by almost 2°C during the last 11.5 ka (Fig. 9). Winter temperature shows a smaller variability, decreasing less than 1°C over the whole period, while the simulated annual mean temperature decreases by around 1°C over the course of the Holocene. Overall, in ORBGHG the simulated temperatures evolution in Siberia is of a similar scale to that of NW Europe.

The difference in simulated temperatures between ORBGHG and OGIS_FWF-v1 varies in summer and winter. On the one hand, the simulated summer temperature in OGIS_FWF-v1 is generally similar to that in ORBGHG with the exception of a small warming of 0.7°C before 10 ka, leading to a weak warm maximum. On the other hand, simulated winter temperature in OGIS_FWF-v1 is around 2°C lower than in ORBGHG before 7 ka. In OGIS_FWF-v1, winter temperature over Siberia stays lower and relatively stable level until 7 ka, followed by a rapid increase over the next 500 yrs after which it follows ORBGHG. Consequently, the early Holocene linear warming rate is much more prominent in winter (0.68°C ka⁻¹) than in summer (0.42°C ka⁻¹). The evolution of the annual mean temperature is intermediate between these two seasons. It is clear that the seasonality in Siberia also decreases from the early Holocene onwards. The simulated temperatures evolution in OGIS_FWF-v2 generally follows that of OGIS_FWF-v1.

Effects of melting ice sheets and orbital forcing

Y. Zhang et al.

Title Page

Abstract

Introduction

Conclusions

References

Tables

Figures



Back

Close

Full Screen / Esc

Printer-friendly Version

Interactive Discussion



4 Discussion

In order to evaluate our results, we briefly compare the simulations with proxy-based reconstructions, followed by an analysis of the mechanism behind the noted temperature patterns. After that, the impact of freshwater forcing will be discussed in more detail based on our transient experiments.

4.1 Comparison of simulations with proxy records

In Europe, climate reconstructions based biological proxies, including pollen and chironomids, consistently show that early Holocene's summer and winter climates were 0.5–2 and 1–3 °C cooler than at present (Mauri et al., 2015). Even though according to reconstructions of Mauri et al. (2015), the climate at 11 ka was warmer than the present in northernmost Scandinavia, the Alps and the Anatolian plateau mountain, this warmer climate is not consistent with the chironomid-based reconstructions for Scandinavia and the Alps (Heiri et al., 2104). Additional geochemical evidence from lake sediments and speleothems, for example in Northern Norway also reflect cooler climate in the early Holocene than in the pre-industrial era (Lauritzen and Lundberg, 1999; Balascio and Bradley, 2012). This overall cool climate in reconstructions generally matches with our simulation OGIS11.5 that shows a lower annual temperature at 11.5 ka than the pre-industrial run.

In Siberia, proxies from lake sediments suggest different patterns from the east to the west. Geochemical proxies together with diatom and pollen data indicate lower temperatures in the early Holocene over eastern Siberia. For example, diatom and pollen assemblages and geochemical measurements (e.g. total organic carbon and concentration of pyrite) in lake sediments near the Lena River (Laing et al., 1999; Muller et al., 2009; Biskaborn et al., 2012; Klemm et al., 2013; Tarasov et al., 2013) consistently reflect a cooler climate than present day (Biskaborn et al., 2012). In western Siberia, reconstructions extending back to the early Holocene are relatively sparse. The available pollen-based reconstructions from Kharinei Lake and Lake Tumbulovaty, on the

Effects of melting ice sheets and orbital forcing

Y. Zhang et al.

[Title Page](#)

[Abstract](#)

[Introduction](#)

[Conclusions](#)

[References](#)

[Tables](#)

[Figures](#)



[Back](#)

[Close](#)

[Full Screen / Esc](#)

[Printer-friendly Version](#)

[Interactive Discussion](#)



Effects of melting ice sheets and orbital forcing

Y. Zhang et al.

Title Page

Abstract

Introduction

Conclusions

References

Tables

Figures



Back

Close

Full Screen / Esc

Printer-friendly Version

Interactive Discussion



western side of the Ural Mountains, suggest similar summer temperatures in the early Holocene (within 1 °C deviations) as today (Salonen et al., 2011). By contrast, our simulation OGIS11.5 indicates that the annual mean temperature was about 1.5 °C lower at 11.5 ka than the pre-industrial era over the whole region, and is thus in better agreement with reconstructions in the eastern than in the western within Siberia.

In the Arctic, we compare our result with the sea-ice cover reconstructions due to the scarcity of temperature reconstructions extending back to the early Holocene. Dinocyst-based reconstructions reveal diverse patterns of sea ice during the early Holocene among different parts of the Arctic: over the Barents Sea, a higher sea-ice concentration in the early Holocene than the recent period implies a cooler early Holocene (de Vernal et al., 2013), while only a minor sea ice change is found in the Canadian Arctic where the sea ice concentration is high throughout the whole Holocene. In addition, pollen-based temperature reconstructions from Melville Island (NW Canadian Arctic) show a 0.3 °C lower July temperature (Peros et al., 2010), and $\delta^{18}\text{O}$ together with direct borehole temperature measurements from Greenland ice cores indicate about 3 °C cooler climate than the present (Dahl-Jensen et al., 1998; Vinther et al., 2008). Overall, these proxies suggest cooler conditions in the Barents Sea (eastern Arctic) and Greenland (Peros et al., 2010; de Vernal et al., 2013; Dahl-Jensen et al., 1998; Vinther et al., 2008), agreeing roughly with the simulated lower temperatures in our OGIS11.5 simulation than in PI. However, the reconstructed temperature signals from the Canadian Arctic are inconclusive (de Vernal et al., 2013), while our OGIS11.5 simulation reflects an overall warmer climate in the west and cooler in the east.

In addition, diatom assemblages, planktonic foraminiferal $\delta^{18}\text{O}$ and Mg/Ca data from the N Atlantic Ocean also indicate a slightly lower sea surface temperature (Came et al., 2007; Berner et al., 2008) in the earliest Holocene than at the present, which is in line with the simulated negative temperature anomalies in OGIS11.5. The estimated sea-ice coverage based on dinocyst assemblages from the Greenland Sea (MSM 712 core) suggests a minor negative sea ice concentration anomaly during 9–6 ka relative

to the most recent 3 ka (de Vernal et al., 2013). This would support our simulated warmer conditions over the Greenland Sea if we assume that this negative sea ice concentration anomaly could extend back to 11.5 ka.

In North America, the proxies indicate significantly different patterns in the east and the west. In Central Beringia, the warmer summer during early Holocene is reflected by the peat accumulation and appearance of *Pinus pumila* in pollen assemblages (Anderson et al., 1988; Lozhkin et al., 2001; Jones and Yu, 2010). In Alaska, the higher-than-present temperature between 11.5 and 9 ka is reflected by northward expansion of animal and plant taxa (Kaufman et al., 2004). This warmer early Holocene in Alaska is also indicated by the earlier initiation of HTM (from 11 to 10 ka) represented by the compiled multi-proxy reconstructions (Kaufman et al., 2004). By contrast, in Eastern Canada the later initiation and termination of HTM (6 and 3 ka, respectively, or even later in some areas) imply lower temperatures during the early Holocene (Kaufman et al., 2004), even though the temperature reconstructions in this region are limited by the fact that the region was covered by the LIS in the early Holocene. This thermal contrast within the same continent agrees well with our simulation OGIS11.5 in which warmer temperatures are simulated in Alaska, while a much cooler climate is found over Canada. Therefore, our simulation with full forcings (OGIS11.5) is able to capture the main features in temperatures that are commonly recorded by the proxies, and has better agreement with proxies in places where the density of reconstructions is relatively high (e.g. in Europe) than in places where reconstructions are sparse (e.g. western Siberia).

As for the temperatures evolution, the multi-proxy reconstructions show that the Holocene was generally characterized by an initial warming and subsequent Holocene warm period over most of regions (Kaufman et al., 2004; Vinther et al., 2008; Brooks et al., 2012; Shakun et al., 2012). These features match with our simulation in which the temperatures rise during the early Holocene, reach a warm period and then gradually decrease to the present, with the exception of Alaska. Concerning the rate of warming in the early Holocene, $\delta^{18}\text{O}$ data and borehole temperature measurements

CPD

11, 5345–5399, 2015

Effects of melting ice sheets and orbital forcing

Y. Zhang et al.

Title Page

Abstract

Introduction

Conclusions

References

Tables

Figures



Back

Close

Full Screen / Esc

Printer-friendly Version

Interactive Discussion



Effects of melting ice sheets and orbital forcing

Y. Zhang et al.

Title Page

Abstract

Introduction

Conclusions

References

Tables

Figures



Back

Close

Full Screen / Esc

Printer-friendly Version

Interactive Discussion



from Greenland suggest a large overall warming rate ($0.8\text{--}1.9^\circ\text{C ka}^{-1}$), while in Siberia and Norway, most reconstructions indicate that this rate is less than 1°C ka^{-1} (Dahl-Jensen et al., 1998; Lauritzen and Lundberg, 1999; Johnsen et al., 2001; Vinther et al., 2009; Klemm et al., 2013; Tarasov et al., 2013). These proxy-indicated warming rates are similar to the rates suggested by our simulation. However, further comparison of these warming rates (region by region) with proxy records is hindered by the scarcity of proxy data in some areas (e.g. the Arctic) and the large variation between proxy reconstructions.

4.2 Mechanism of climate response to forcings

It is obvious that the spatial patterns of climate response at the onset of Holocene can be attributed to the various dominant forcings in different areas. Orbitally induced insolation is one of important driving factors for the early Holocene temperatures. For instance, in Alaska, the higher temperature is primarily determined by the orbitally induced positive insolation anomaly, which is also reflected by a relatively small variation between the simulations OG11.5 and OGIS11.5. Apart from the insolation, the anomalous atmospheric circulation caused by the remnant LIS, which is indicated by the 800 hPa Geopotential height (Fig. 11), also played an important role (e.g. caused the slightly warmer climate) in Alaska. Over the cold LIS surface, the air descends, creating a high surface pressure anomaly that produces a clockwise flow anomaly at the surface. This induces stronger southerly winds over Alaska in OGIS11.5 than in OG11.5 that advected relatively warm air from the South.

The strong influence of ice sheets on early Holocene temperatures has been found in previous modelling studies which revealed the cooling impact of the LIS and thus delaying the HTM (Renssen et al., 2009, 2012). The simulated lower summer temperatures over the eastern part of N America and NW Europe in our simulation OGIS11.5 compared to the preindustrial run is the result of such cooling effect induced by ice sheets, which fully overwhelms the warming effect of the positive summer insolation

Effects of melting ice sheets and orbital forcing

Y. Zhang et al.

Title Page

Abstract

Introduction

Conclusions

References

Tables

Figures



Back

Close

Full Screen / Esc

Printer-friendly Version

Interactive Discussion



anomaly. The ice sheets' cooling effect, on a local scale, can be partly explained by the enhanced albedo over the ice sheets and by the climate's high sensitivity to land albedo change (Romanova et al., 2006). Indeed, the summer surface albedo over the ice sheets exceeds 0.8, and is thus much higher than the albedo of ice-free surfaces with values varying from 0.1 in mid-latitudes to 0.5 in high latitudes, depending on the vegetation type and the fractional snow cover (Fig. 10). Apart from the enhanced surface albedo, the orographic effect of the ice sheets can influence the climate as well, as the elevation is raised by several hundred metres with a maximum of up to 2000 m in the center of LIS. Actually, the previous studies have reported that the ice-sheet related elevation change has a notable effect on the atmosphere during the LGM, as it sets many features of surface pressure field, including the location of the subtropical highs and subpolar lows (Felzer et al., 1996; Justino and Peltier, 2005; Langen and Vinther, 2009). On the local scale, the glacial anticyclones over the ice sheets resulted from the descent of cool air from the upper layer cause the cooling of surface temperature (Felzer et al., 1996). At the onset of the Holocene, although the ice sheets were much smaller than during the LGM, they still had an identifiable impact in atmosphere. For instance, the descending air over the LIS created the anomalously high surface pressure and thus the changes in wind directions that influence the surrounding areas (Fig. 11), as already noted above. From the record side, the abrupt transitions of deuterium excess and the considerable reduction in dust concentration in the NGRIP ice core at the very beginning of Holocene also indicate a change in atmospheric circulation near the N Atlantic (Steffensen et al., 2008). The enhanced elevation over ice sheets also has a few degree cooling effect on temperature on a local scale if we take the environmental lapse rate into account.

The corresponding changes in vegetation and landcover in the early Holocene contribute to climate change especially over ecotonal regions. Modelling studies suggest that deforestation in boreal regions decrease the regional temperature by almost up to 1 °C due to an increase in surface albedo and related positive feedbacks (biogeophysical effects) (Levis et al., 1999; Claussen et al., 2001; Liu et al., 2006). If we take Siberia

Effects of melting ice sheets and orbital forcing

Y. Zhang et al.

[Title Page](#)

[Abstract](#)

[Introduction](#)

[Conclusions](#)

[References](#)

[Tables](#)

[Figures](#)



[Back](#)

[Close](#)

[Full Screen / Esc](#)

[Printer-friendly Version](#)

[Interactive Discussion](#)



as an example, the summer climate is cooler in OGIS11.5 than the preindustrial over Siberia, which can be associated with the overall higher summer albedo in simulation OGIS11.5 (some areas are up to 0.28) than in the PI (lower than 0.22). This is a consequence of the more southward extended tundra or/and bare ground which has a higher albedo than boreal forest at 11.5 ka compared with 0 ka. Apart from albedo-related feedbacks between boreal forest and tundra, the relatively small insolation deviation from the present over central Siberia also contributes to lower annual (0.5–1.5 °C) and winter (0.5–2 °C) temperatures at that time.

At the same time, meltwater release and sea-ice related changes in the high-latitude oceans also have a footprint in the early Holocene climate. The simulation with full forcings produced a clear slowdown of the AMOC in the N Atlantic with the maximum value decreasing by more than 3 Sv. It also reflected a shallower overturning circulation at 11.5 ka compared to the preindustrial era as a response to meltwater generated from the deglaciation of ice sheets (Fig. 12). This slowdown in ocean circulation is consistent with the planktonic foraminifera records from the Arctic Ocean and Fram Strait which suggest reduced northward heat transport through ocean circulation (Thornalley et al., 2009). This led to a slightly lower temperature in high latitudes (western part of Arctic Ocean) at 11.5 ka than in the preindustrial period. However, it is worth noticing that the temperature decrease is not linear with the amount of northward transport heat since the sea-ice feedbacks further reinforce this change (Roche et al., 2007). Actually, sea ice coverage in OGIS11.5 is much more extensive over Davis Strait (N Labrador Sea) than in OG11.5 (Fig. 13) implying that positive feedbacks involving sea ice were active (Renssen et al., 2005). As for the Greenland Sea warming, it can be attributed to enhanced convective activity here associated with the deep water formation, releasing oceanic heat to the atmosphere. This enhanced convective activity is caused by the shift of deep water formation from the east Greenland Sea to the west, which is induced by the freshwater discharge from ice sheets melting. Overall, the net response of climate represents the combined forcings, significantly depending on the

et al., 2005). Apart from the intensity and duration, the response of ocean circulation to freshwater also depends on the location where this freshwater is released. For instance, it is more sensitive to the release of freshwater at the eastern Norwegian Sea than at the St. Lawrence River outlet since the former is closer to the main site with NADW formation (Roche et al., 2010). This is consistent with the previous study of Blaschek and Renssen (2103), in which they found that freshwater from the GIS did have a non-ignorable impact on Nordic seas and its circulation, even though the total amount is minor. This location-dependence sensitivity could also explain why the AMOC is weaker in OGIS_FWF_v2 than in OGIS_FWF-v1.

In NW Europe, the OGIS_FWF-v1 produced two peaks of temperature, around 10 and 7 ka. High temperatures at 7 ka are also recorded in proxy-based reconstructions. However, no warm peak at 10 ka can be observed in pollen-based reconstructions, which suggests a cooler climate at 10 ka than present in Europe (Mauri et al., 2015). In contrast to OGIS_FWF-v1, the simulation with updated freshwater (OGIS_FWF-v2) produced a warming trend, which is consistent with a highest temperature around 7 ka. Moreover, the OGIS_FWF-v1 produced a temperature decrease between two peaks while the proxies suggest rapid temperature increase at the beginning followed by the gradual warming (Brooks et al., 2012). Meanwhile, given the albedo's influences on temperature (Romanova et al., 2006), the albedo in the model has been checked and it turns out that the albedo value in the model is consistent with the vegetation of dwarf shrub and herb over Scandinavia at that time (Allen et al., 2010). Therefore, from the viewpoint of temperature evolutions, OGIS_FWF-v2 is more realistic than OGIS_FWF-v1, implying a faster thinning of GIS as suggested by Vinther et al. (2009) and, correspondingly, larger meltwater release in early period would be more realistic.

5 Conclusions

We performed both equilibrium and transient simulations by employing the LOVECLIM climate model in order to explore the spatial patterns of the climate response to forcing

Effects of melting ice sheets and orbital forcing

Y. Zhang et al.

[Title Page](#)

[Abstract](#)

[Introduction](#)

[Conclusions](#)

[References](#)

[Tables](#)

[Figures](#)



[Back](#)

[Close](#)

[Full Screen / Esc](#)

[Printer-friendly Version](#)

[Interactive Discussion](#)



at the onset of Holocene and the temperatures evolution over the last 11.5 ka. In our analysis, we focus on three research questions.

1. What are the main spatial characteristics of temperature at the onset of the Holocene?

The temperatures at 11.5 ka are regionally heterogenous, which is represented by a range of annually negative anomalies over many areas and highlighted by higher value in Alaska, compared with the preindustrial era. In eastern N America and NW Europe, the climate reached the maximum cooling with temperature anomalies of -2 to -5°C relative to 0 ka throughout the year. For Siberia, the temperatures were 0.5 – 3 and 1.5 – 3°C lower in winter and annual average, and summer temperature showed a small deviation (between $+0.5$ to -1.5°C) compared to the preindustrial period. In the eastern part of Arctic Ocean (over Barents Sea, Kara Sea and Laptev Sea), the summer temperature anomaly (between -0.5 and $+0.5^{\circ}\text{C}$) was also small, and annual temperatures were 0.5 – 2°C lower than at 0 ka. In addition, the climate over the N Labrador Sea and the N Atlantic Ocean were 0.5 – 3°C cooler than the preindustrial during the whole year. In contrast to cooler condition in other areas, the temperatures in all seasons in Alaska were 1.5 – 3°C higher than pre-industrial period.

2. What is the role of forcings, especially ice sheet decay, in shaping these characteristics and what are possible other mechanisms?

The relatively cold climate at 11.5 ka in eastern N America and NW Europe is a consequence of the ice sheets' cooling effects that overwhelm the warming impact of the positive insolation anomaly. In particular, the enhanced surface albedo of the ice and the orographic effects were important for the cold conditions. For Siberia, a small summer temperature anomaly in response to positive insolation anomaly was surpassed by the cooling effect of the high albedo associated with tundra which was more extensive in early Holocene than at the present. The overall lower winter and annual temperatures can be attributed to both vegetation-

Effects of melting ice sheets and orbital forcing

Y. Zhang et al.

Title Page

Abstract

Introduction

Conclusions

References

Tables

Figures



Back

Close

Full Screen / Esc

Printer-friendly Version

Interactive Discussion



Overall, our results demonstrate a large spatial variability in the climate response to diverse forcings, both in terms of temperature distribution at the onset of the Holocene and in the early Holocene warming.

**The Supplement related to this article is available online at
doi:10.5194/cpd-11-5345-2015-supplement.**

References

- Abe-Ouchi, A., Saito, F., Kawamura, K., Raymo, M. E., Okuno, J., Takahashi, K., and Blatter, H.: Insolation-driven 100,000-year glacial cycles and hysteresis of ice-sheet volume, *Nature*, 500, 190–193, doi:10.1038/nature12374, 2013.
- Allen, J. R. M., Hickler, T., Singarayer, J. S., Sykes, M. T., Valdes, P. J., and Huntley, B.: Last glacial vegetation of northern Eurasia, *Quaternary Sci. Rev.*, 29, 2604–2618, doi:10.1016/j.quascirev.2010.05.031, 2010.
- Anderson, P. M., Reanier, R. E., and Brubaker, L. B.: Late quaternary vegetational history of the Black River region in northeastern Alaska, *Can. J. Earth Sci.*, 25, 84–94, 1988.
- Anderson, R. F., Ali, S., Bradtmiller, L. I., Nielsen, S. H. H., Fleisher, M. Q., Anderson, B. E., and Burckle, L. H.: Wind-driven upwelling in the Southern Ocean and the deglacial rise in atmospheric CO₂, *Science*, 323, 1443–1448, doi:10.1126/science.1167441, 2009.
- Anklin, M., Barnola, J. M., Beer, J., Blunier, T., Chappellaz, J., Clausen, H. B., Dahljensen, D., Dansgaard, W., Deangelis, M., Delmas, R. J., Duval, P., Fratta, M., Fuchs, A., Fuhrer, K., Gundestrup, N., Hammer, C., Iversen, P., Johnsen, S., Jouzel, J., Kipfstuhl, J., Legrand, M., Lorius, C., Maggi, V., Miller, H., Moore, J. C., Oeschger, H., Orombelli, G., Peel, D. A., Raisbeck, G., Raynaud, D., Schotthvidberg, C., Schwander, J., Shoji, H., Souchez, R., Stauffer, B., Steffensen, J. P., Stievenard, M., Sveinbjornsdottir, A., Thorsteinsson, T., and Wolff, E. W.: Climate instability during the last interglacial period recorded in the GRIP ice core, *Nature*, 364, 203–207, 1993.
- Balascio, N. L. and Bradley, R. S.: Evaluating Holocene climate change in northern Norway using sediment records from two contrasting lake systems, *J. Paleolimnol.*, 48, 259–273, doi:10.1007/s10933-012-9604-7, 2012.

Effects of melting ice sheets and orbital forcing

Y. Zhang et al.

Title Page

Abstract

Introduction

Conclusions

References

Tables

Figures



Back

Close

Full Screen / Esc

Printer-friendly Version

Interactive Discussion



Effects of melting ice sheets and orbital forcing

Y. Zhang et al.

Title Page

Abstract

Introduction

Conclusions

References

Tables

Figures



Back

Close

Full Screen / Esc

Printer-friendly Version

Interactive Discussion



- Berger, A. L.: Long-term variations of daily insolation and Quaternary climatic changes, *J. Atmos. Sci.*, 35, 2362–2367, 1978.
- Berger, A.: Milankovitch theory and climate, *Rev. Geophys.*, 26, 624–657, 1988.
- Berner, K. S., Koç, N., Divine, D., Godtliebsen, F., and Moros, M.: A decadal-scale Holocene sea surface temperature record from the subpolar North Atlantic constructed using diatoms and statistics and its relation to other climate parameters, *Paleoceanography*, 23, PA2210, doi:10.1029/2006pa001339, 2008.
- Bigelow, N. H., Brubaker, L. B., Edwards, M. E., Harrison, S. P., Prentice, I. C., Anderson, P. M., Andreev, A. A., Bartlein, P. J., Christensen, T. R., Cramer, W., Kaplan, J. O., Lozhkin, A. V., Matveyeva, N. V., Murray, D. F., McGuire, A. D., Razzhivin, V. Y., Ritchie, J. C., Smith, B., Walker, D. A., Gajewski, K., Wolf, V., Holmqvist, B. H., Igarashi, Y., Kremenetskii, K., Paus, A., Pisaric, M. F. J., and Volkova, V. S.: Climate change and Arctic ecosystems: vegetation changes north of 55° N between the last glacial maximum, mid-Holocene, and present, *J. Geophys. Res.*, 108, 8170, doi:10.1029/2002JD002558, 2003.
- Birks, H. H.: South to north: contrasting late-glacial and early-Holocene climate changes and vegetation responses between south and north Norway, *Holocene*, 25, 37–52, doi:10.1177/0959683614556375, 2015.
- Biskaborn, B. K., Herzschuh, U., Bolshiyarov, D., Savelieva, L., and Diekmann, B.: Environmental variability in northeastern Siberia during the last ~13,300 years inferred from lake diatoms and sediment–geochemical parameters, *Palaeogeog. Paleoclim. Palaeoecol.*, 329/330, 22–36, doi:10.1016/j.palaeo.2012.02.003, 2012.
- Blaschek, M. and Renssen, H.: The Holocene thermal maximum in the Nordic Seas: the impact of Greenland Ice Sheet melt and other forcings in a coupled atmosphere–sea-ice–ocean model, *Clim. Past*, 9, 1629–1643, doi:10.5194/cp-9-1629-2013, 2013.
- Bond, G., Broecker, W., Johnsen, S., McManus, J., Labeyrie, L., Jouzel, J., and Bonani, G.: Correlations between climate records from North Atlantic sediments and Greenland ice, *Nature*, 365, 143–147, doi:10.1038/365143a0, 1993.
- Brooks, S. J. and Birks, H. J. B.: Chironomid-inferred Late-glacial and early Holocene mean July air temperatures for Krakenes Lake, western Norway, *J. Paleolimnol.*, 23, 77–89, 2000.
- Brooks, S. J., Matthews, I. P., Birks, H. H., and Birks, H. J. B.: High resolution Lateglacial and early-Holocene summer air temperature records from Scotland inferred from chironomid assemblages, *Quaternary Sci. Rev.*, 41, 67–82, doi:10.1016/j.quascirev.2012.03.007, 2012.

Effects of melting ice sheets and orbital forcing

Y. Zhang et al.

[Title Page](#)

[Abstract](#)

[Introduction](#)

[Conclusions](#)

[References](#)

[Tables](#)

[Figures](#)



[Back](#)

[Close](#)

[Full Screen / Esc](#)

[Printer-friendly Version](#)

[Interactive Discussion](#)



- Brovkin, V., Ganopolski, A., and Svirezhev, Y.: A continuous climate-vegetation classification for use in climate-biosphere studies, *Ecol. Model.*, 101, 251–261, 1997.
- Buizert, C., Gkinis, V., Severinghaus, J. P., He, F., Lecavalier, B. S., Kindler, P., Leuenberger, M., Carlson, A. E., Vinther, B., Masson-Delmotte, V., White, J. W. C., Liu, Z., Otto-Bliesner, B., and Brook, E. J.: Greenland temperature response to climate forcing during the last deglaciation, *Science*, 345, 1177–1180, doi:10.1126/science.1254961, 2014.
- Came, R. E., Oppo, D. W., and McManus, J. F.: Amplitude and timing of temperature and salinity variability in the subpolar North Atlantic over the past 10 k.y., *Geology*, 35, 315–318, doi:10.1130/g23455a.1, 2007.
- CAPE project members: Holocene paleoclimate data from the arctic: testing models of global climate change, *Quaternary Sci. Rev.*, 20, 1275–1287, doi:10.1016/S0277-3791(01)00010-5, 2001.
- Carlson, A. E., Winsor, K., Ullman, D. J., Brook, E., Rood, D. H., Axford, Y., Le Grande, A. N., Anslow, F., and Sinclair, G.: Earliest Holocene south Greenland ice-sheet retreat within its late-Holocene extent, *Geophys. Res. Lett.*, 41, 5514–5521, doi:10.1002/2014GL060800, 2014.
- Claussen, M., Brovkin, V., and Ganopolski, A.: Biogeophysical versus biogeochemical feedbacks of large-scale land cover change, *Geophys. Res. Lett.*, 28, 1011–1014, doi:10.1029/2000gl012471, 2001.
- Dahl-Jensen, D., Mosegaard, K., Gundestrup, N., Clow, G. D., Johnsen, S. J., Hansen, A. W., and Balling, N.: Past temperatures directly from the Greenland ice sheet, *Science*, 282, 268–271, 1998.
- Dansgaard, W., Johnsen, S. J., Clausen, H. B., Dahl-Jensen, D., Gundestrup, N. S., Hammer, C. U., Hvidberg, C. S., Steffensen, J. P., Sveinbjornsdottir, A. E., Jouzel, J., and Bond, G.: Evidence for general instability of past climate from a 250 kyr ice-core record, *Nature*, 364, 218–220, 1993.
- de Vernal, A., Hillaire-Marcel, C., Rochon, A., Fréchet, B., Henry, M., Solignac, S., and Bonnet, S.: Dinocyst-based reconstructions of sea ice cover concentration during the Holocene in the Arctic Ocean, the northern North Atlantic Ocean and its adjacent seas, *Quaternary Sci. Rev.*, 79, 111–121, doi:10.1016/j.quascirev.2013.07.006, 2013.
- Denton, G. H., Anderson, R. F., Toggweiler, J. R., Edwards, R. L., Schaefer, J. M., and Putnam, A. E.: The last glacial termination, *Science*, 328, 1652–1656, doi:10.1126/science.1184119, 2010.

Effects of melting ice sheets and orbital forcing

Y. Zhang et al.

Title Page

Abstract

Introduction

Conclusions

References

Tables

Figures



Back

Close

Full Screen / Esc

Printer-friendly Version

Interactive Discussion



- Dyke, A. S., Moore, A., and Robertson, L.: Deglaciation of North America, Open-file report-geological survey of Canada, Geological Survey of Canada, Ottawa, 2003.
- Fang, K., Morris, J. L., Salonen, J. S., Miller, P. A., Renssen, H., Sykes, M. T., and Seppä, H.: How robust are Holocene treeline simulations? A model-data comparison in the European Arctic treeline region, *J. Quaternary Sci.*, 28, 595–604, doi:10.1002/jqs.2654, 2013.
- Felzer, B., Oglesby, R. J., Webb, T., and Hyman, D. E.: Sensitivity of a general circulation model to changes in Northern Hemisphere ice sheets, *J. Geophys. Res.-Atmos.*, 101, 19077–19092, doi:10.1029/96JD01219, 1996.
- Fichefet, T. and Maqueda, M. A. M.: Sensitivity of a global sea ice model to the treatment of ice thermodynamics and dynamics, *J. Geophys. Res.*, 102, 12609–12646, doi:10.1029/97jc00480, 1997.
- Ganopolski, A., Kubatzki, C., Claussen, M., Brovkin, V., and Petoukhov, V.: The influence of vegetation-atmosphere–ocean interaction on climate during the mid-Holocene, *Science*, 280, 1916–1919, 1998.
- Ganopolski, A., Calov, R., and Claussen, M.: Simulation of the last glacial cycle with a coupled climate ice-sheet model of intermediate complexity, *Clim. Past*, 6, 229–244, doi:10.5194/cp-6-229-2010, 2010.
- Goosse, H. and Fichefet, T.: Importance of ice–ocean interactions for the global ocean circulation: a model study, *J. Geophys. Res.*, 23, 337–355, doi:10.1029/1999jc900215, 1999.
- Goosse, H., Brovkin, V., Fichefet, T., Haarsma, R., Huybrechts, P., Jongma, J., Mouchet, A., Selten, F., Barriat, P.-Y., Campin, J.-M., Deleersnijder, E., Driesschaert, E., Goelzer, H., Janssens, I., Loutre, M.-F., Morales Maqueda, M. A., Opsteegh, T., Mathieu, P.-P., Munhoven, G., Pettersson, E. J., Renssen, H., Roche, D. M., Schaeffer, M., Tartinville, B., Timmermann, A., and Weber, S. L.: Description of the Earth system model of intermediate complexity LOVECLIM version 1.2, *Geosci. Model Dev.*, 3, 603–633, doi:10.5194/gmd-3-603-2010, 2010.
- Grootes, P. M., Stuiver, M., White, J. W. C., Johnsen, S., and Jouzel, J.: Comparison of oxygen isotope records from the GISP2 and GRIP Greenland ice cores, *Nature*, 366, 552–554, 1993.
- Hald, M., Andersson, C., Ebbesen, H., Jansen, E., Klitgaard-Kristensen, D., Risebrobakken, B., Salomonsen, G. R., Sarnthein, M., Sejrup, H. P., and Telford, R. J.: Variations in temperature and extent of Atlantic Water in the northern North Atlantic during the Holocene, *Quaternary Sci. Rev.*, 26, 3423–3440, doi:10.1016/j.quascirev.2007.10.005, 2007.

Effects of melting ice sheets and orbital forcing

Y. Zhang et al.

Title Page

Abstract

Introduction

Conclusions

References

Tables

Figures



Back

Close

Full Screen / Esc

Printer-friendly Version

Interactive Discussion



- Heiri, O., Brooks, S. J., Renssen, H., Bedford, A., Hazekamp, M., Ilyashuk, B., Jeffers, E. S., Lang, B., Kirilova, E., Kuiper, S., Millet, L., Samartin, S., Toth, M., Verbruggen, F., Watson, J. E., van Asch, N., Lammertsma, E., Amon-Veskimeister, L., Birks, H. H., Birks, H. J. B., Mortensen, M. F., Hoek, W., Magyari, E., Muñoz Sobrino, C., Seppä, H., Tinner, W., Tonkov, S., Veski, S., and Lotter, A. F.: Validation of climate model-inferred regional temperature change for late-glacial Europe, *Nature Communications*, 5, 1–7, doi:10.1038/ncomms5914, 2014.
- Hofer, D., Raible, C. C., Merz, N., Dehnert, A., and Kuhlemann, J.: Simulated winter circulation types in the North Atlantic and European region for preindustrial and glacial conditions, *Geophys. Res. Lett.*, 39, L15805, doi:10.1029/2012GL052296, 2012.
- Jennings, A., Andrews, J., Pearce, C., Wilson, L., and Ólfasdóttir, S.: Detrital carbonate peaks on the Labrador shelf, a 13–7 ka template for freshwater forcing from the Hudson Strait outlet of the Laurentide Ice Sheet into the subpolar gyre, *Quaternary Sci. Rev.*, 107, 62–80, doi:10.1016/j.quascirev.2014.10.022, 2015.
- Johnsen, S. J., Dahl-Jensen, D., Gundestrup, N., Steffensen, J. P., Clausen, H. B., Miller, H., Masson-Delmotte, V., Sveinbjornsdottir, A. E., and White, J.: Oxygen isotope and palaeotemperature records from six Greenland ice-core stations: Camp Century, Dye-3, GRIP, GISP2, Renland and NorthGRIP, *J. Quaternary Sci.*, 16, 299–307, doi:10.1002/jqs.622, 2001.
- Jones, M. C. and Yu, Z.: Rapid deglacial and early Holocene expansion of peatlands in Alaska, *P. Natl. Acad. Sci. USA*, 107, 7347–7352, doi:10.1073/pnas.0911387107, 2010.
- Justino, F. and Peltier, W. R.: The glacial North Atlantic oscillation, *Geophys. Res. Lett.*, 32, L21803, doi:10.1029/2005GL023822, 2005.
- Kandiano, E. S., Bauch, H. A., and Müller, A.: Sea surface temperature variability in the North Atlantic during the last two glacial–interglacial cycles: comparison of faunal, oxygen isotopic, and Mg/Ca-derived records, *Palaeogeogr. Paleoclimatol.*, 204, 145–164, doi:10.1016/s0031-0182(03)00728-4, 2004.
- Kaufman, D. S., Ager, T. A., Anderson, N. J., Anderson, P. M., Andrews, J. T., Bartlein, P. T., Brubaker, L. B., Coats, L. L., Cwynar, L. C., Duvall, M. L., Dyke, A. S., Edwards, M. E., Eisner, W. R., Gajewski, K., Geirsdottir, A., Hu, F. S., Jennings, A. E., Kaplan, M. R., Kerwin, M. W., Lozhkin, A. V., MacDonald, G. M., Miller, G. H., Mock, C. J., Oswald, W. W., Otto-Bliesner, B. L., Porinchu, D. F., Ruhland, K., Smol, J. P., Steig, E. J., and Wolfe, B. B.: Holocene thermal maximum in the western Arctic (0–180° W), *Quaternary Sci. Rev.*, 23, 529–560, doi:10.1016/j.quascirev.2003.09.007, 2004.

Effects of melting ice sheets and orbital forcing

Y. Zhang et al.

[Title Page](#)

[Abstract](#)

[Introduction](#)

[Conclusions](#)

[References](#)

[Tables](#)

[Figures](#)



[Back](#)

[Close](#)

[Full Screen / Esc](#)

[Printer-friendly Version](#)

[Interactive Discussion](#)



Klemm, J., Herzschuh, U., Pisaric, M. F. J., Telford, R. J., Heim, B., and Pestryakova, L. A.: A pollen-climate transfer function from the tundra and taiga vegetation in Arctic Siberia and its applicability to a Holocene record, *Palaeogeogr. Paleocl.*, 386, 702–713, doi:10.1016/j.palaeo.2013.06.033, 2013.

5 Koerner, R. M. and Fisher, D. A.: A record of Holocene summer climate from a Canadian High Arctic ice core, *Nature*, 343, 630–631, 1990.

Lambeck, K., Rouby, H., Purcell, A., Sun, Y., and Sambridge, M.: Sea level and global ice volumes from the Last Glacial Maximum to the Holocene, *P. Natl. Acad. Sci. USA*, 111, 15296–15303, 2014.

10 Laing, T. E., Rühland, K. M., and Smol, J. P.: Past environmental and climatic changes related to tree-line shifts inferred from fossil diatoms from a lake near the Lena River Delta, Siberia, *Holocene*, 9, 547–557, 1999.

Langen, P. L. and Vinther, B. M.: Response in atmospheric circulation and sources of Greenland precipitation to glacial boundary conditions, *Clim. Dynam.*, 32, 1035–1054, doi:10.1007/s00382-008-0438-y, 2009.

15 Lauritzen, S. E. and Lundberg, J.: Calibration of the speleothem delta function: an absolute temperature record for the Holocene in northern Norway, *Holocene*, 9, 659–669, 1999.

Levis, S., Foley, J. A., and Pollard, D.: CO₂, climate, and vegetation feedbacks at the Last Glacial Maximum, *J. Geophys. Res.*, 104, 31191–31198, doi:10.1029/1999jd900837, 1999.

20 Licciardi, J. M., Teller, J. T., and Clark, P. U.: Freshwater routing by the Laurentide Ice Sheet during the last deglaciation, mechanism of global climate change at millennial time scales, *Geoph. Monog. Series*, 112, 177–201, 1999.

Liu, Z., Notaro, M., Kutzbach, J. E., and Liu, N.: Assessing global vegetation-climate feedbacks from observations, *J. Climate*, 19, 787–814, doi:10.1175/JCLI3658.1, 2006.

25 Loulergue, L., Schilt, A., Spahni, R., Masson-Delmotte, V., Blunier, T., Lemieux, B., Barnola, J. M., Raynaud, D., Stocker, T. F., and Chappellaz, J.: Orbital and millennial-scale features of atmospheric CH₄ over the past 800,000 years, *Nature*, 453, 383–386, doi:10.1038/nature06950, 2008.

Lozhkin, A. V., Anderson, P. M., Vartanyan, S., Brown, T., Belaya, B., and Kotov, A.: Reconstructions of late Quaternary paleo-environments and modern pollen data from Wrangel Island (northern Chukotka), *Quaternary Sci. Rev.*, 20, 217–233, 2001.

30 Lundqvist, J. and Saarnisto, M.: Summary of project IGCP-253, *Quatern. Int.*, 28, 9–18, 1995.

Effects of melting ice sheets and orbital forcing

Y. Zhang et al.

Title Page

Abstract

Introduction

Conclusions

References

Tables

Figures



Back

Close

Full Screen / Esc

Printer-friendly Version

Interactive Discussion



- MacDonald, G. M., Velichko, A. A., Kremenetski, C. V., Borisova, O. K., Goleva, A. A., Andreev, A. A., Cwynar, L. C., Riding, R. T., Forman, S. L., Edwards, T. W. D., Aravena, R., Hammarlund, D., Szeicz, J. M., and Gattaulin, V. N.: Holocene treeline history and climate change across northern Eurasia, *Quaternary Res.*, 53, 302–311, doi:10.1006/qres.1999.2123, 2000.
- 5 Marchitto, T. M., Lehman, S. J., Ortiz, J. D., Fluckiger, J., and van Geen, A.: Marine radiocarbon evidence for the mechanism of deglacial atmospheric CO₂ rise, *Science*, 316, 1456–1459, doi:10.1126/science.1138679, 2007.
- Martinez-Boti, M. A., Foster, G. L., Chalk, T. B., Rohling, E. J., Sexton, P. F., Lunt, D. J., Pancost, R. D., Badger, M. P., and Schmidt, D. N.: Plio-Pleistocene climate sensitivity evaluated using high-resolution CO₂ records, *Nature*, 518, 49–54, doi:10.1038/nature14145, 2015.
- 10 Mauri, A., Davis, B. A. S., Collins, P. M., and Kaplan, J. O.: The climate of Europe during the Holocene: a gridded pollen-based reconstruction and its multi-proxy evaluation, *Quaternary Sci. Rev.*, 112, 109–127, doi:10.1016/j.quascirev.2015.01.013, 2015.
- Monnin, E., Indermuhle, A., Dallenbach, A., Fluckiger, J., Stauffer, B., Stocker, T. F., Raynaud, D., and Barnola, J.-M.: Atmospheric CO₂ concentrations over the last glacial termination, *Science*, 291, 112–114, doi:10.1126/science.291.5501.112, 2001.
- 15 Müller, S., Tarasov, P. E., Andreev, A. A., and Diekmann, B.: Late Glacial to Holocene environments in the present-day coldest region of the Northern Hemisphere inferred from a pollen record of Lake Billyakh, Verkhoyansk Mts, NE Siberia, *Clim. Past*, 5, 73–84, doi:10.5194/cp-5-73-2009, 2009.
- Occhietti, S., Parent, M., Lajeunesse, P., Robert, F., and Govare, É.: Late Pleistocene-Early Holocene decay of the Laurentide Ice Sheet in Québec-Labrador, *Developments in Quaternary Science*, 15, 601–630, doi:10.1016/b978-0-444-53447-7.00047-7, 2011.
- Opsteegh, J. D., Haarsma, R. J., Selten, F. M., and Kattenberg, A.: ECBILT: a dynamic alternative to mixed boundary conditions in ocean models, *Tellus A*, 50, 348–367, 1998.
- 25 PALAEOSENSE Project Members: Making sense of palaeoclimate sensitivity, *Nature*, 491, 683–691, 2012.
- Pausata, F. S. R., Li, C., Wettstein, J. J., Kageyama, M., and Nisancioglu, K. H.: The key role of topography in altering North Atlantic atmospheric circulation during the last glacial period, *Clim. Past*, 7, 1089–1101, doi:10.5194/cp-7-1089-2011, 2011.
- 30 Peros, M., Gajewski, K., Paull, T., Ravindra, R., and Podrifske, B.: Multi-proxy record of post-glacial environmental change, south-central Melville Island, Northwest Territories, Canada, *Quaternary Res.*, 73, 247–258, doi:10.1016/j.yqres.2009.11.010, 2010.

Effects of melting ice sheets and orbital forcing

Y. Zhang et al.

[Title Page](#)[Abstract](#)[Introduction](#)[Conclusions](#)[References](#)[Tables](#)[Figures](#)[Back](#)[Close](#)[Full Screen / Esc](#)[Printer-friendly Version](#)[Interactive Discussion](#)

- Putkinen, N. and Lunkka, J. P.: Ice stream behaviour and deglaciation of the Scandinavian Ice Sheet in the Kuittijärvi area, Russian Karelia, *Bull. Geol. Soc. Finl.*, 80, 19–37, 2008.
- Rahmstorf, S., Crucifix, M., Ganopolski, A., Goosse, H., Kamenkovich, I., Knutti, R., Lohmann, G., Marsh, R., Mysak, L. A., Wang, Z., and Weaver, A. J.: Thermohaline circulation hysteresis: a model intercomparison, *Geophys. Res. Lett.*, 32, L23605, doi:10.1029/2005gl023655, 2005.
- Rasmussen, S. O., Andersen, K. K., Svensson, A. M., Steffensen, J. P., Vinther, B. M., Clausen, H. B., Siggaard-Andersen, M. L., Johnsen, S. J., Larsen, L. B., Dahl-Jensen, D., Bigler, M., Röthlisberger, R., Fischer, H., Goto-Azuma, K., Hansson, M. E., and Ruth, U.: A new Greenland ice core chronology for the last glacial termination, *J. Geophys. Res.*, 111, D06102, doi:10.1029/2005jd006079, 2006.
- Renssen, H., Goosse, H., and Fichefet, T.: Modeling the effect of freshwater pulses on the early Holocene climate: the influence of high frequency climate variability, *Paleoceanography*, 17, 1020, doi:10.1029/2001PA000649, 2002.
- Renssen, H., Goosse, H., Fichefet, T., Brovkin, V., Driesschaert, E., and Wolk, F.: Simulating the Holocene climate evolution at northern high latitudes using a coupled atmosphere-sea ice-ocean-vegetation model, *Clim. Dynam.*, 24, 23–43, doi:10.1007/s00382-004-0485-y, 2005.
- Renssen, H., Driesschaert, E., Loutre, M. F., and Fichefet, T.: On the importance of initial conditions for simulations of the Mid-Holocene climate, *Clim. Past*, 2, 91–97, doi:10.5194/cp-2-91-2006, 2006.
- Renssen, H., Seppä, H., Heiri, O., Roche, D. M., Goosse, H., and Fichefet, T.: The spatial and temporal complexity of the Holocene thermal maximum, *Nat. Geosci.*, 2, 411–414, doi:10.1038/ngeo513, 2009.
- Renssen, H., Goosse, H., Crosta, X., and Roche, D. M.: Early Holocene Laurentide Ice Sheet deglaciation causes cooling in the high-latitude Southern Hemisphere through oceanic teleconnection, *Paleoceanography*, 25, PA3204, doi:10.1029/2009pa001854, 2010.
- Renssen, H., Seppä, H., Crosta, X., Goosse, H., and Roche, D. M.: Global characterization of the Holocene Thermal Maximum, *Quaternary Sci. Rev.*, 48, 7–19, doi:10.1016/j.quascirev.2012.05.022, 2012.
- Roche, D. M., Renssen, H., Weber, S. L., and Goosse, H.: Could meltwater pulses have been sneaked unnoticed into the deep ocean during the last glacial, *Geophys. Res. Lett.*, 34, L24708, doi:10.1029/2007GL032064, 2007.

Effects of melting ice sheets and orbital forcing

Y. Zhang et al.

Title Page

Abstract

Introduction

Conclusions

References

Tables

Figures



Back

Close

Full Screen / Esc

Printer-friendly Version

Interactive Discussion



Roche, D. M., Wiersma, A. P., and Renssen, H.: A systematic study of the impact of fresh-water pulses with respect to different geographical locations, *Clim. Dynam.*, 34, 997–1013, doi:10.1007/s00382-009-0578-8, 2010.

Romanova, V., Lohmann, G., and Grosfeld, K.: Effect of land albedo, CO₂, orography, and oceanic heat transport on extreme climates, *Clim. Past*, 2, 31–42, doi:10.5194/cp-2-31-2006, 2006.

Ruddiman, W. F.: The early anthropogenic hypothesis: challenges and responses, *Rev. Geophys.*, 45, RG4001, doi:10.1029/2006rg000207, 2007.

Salonen, J. S., Seppä, H., Väliranta, M., Jones, V. J., Self, A., Heikkilä, M., Kultti, S., and Yang, H.: Holocene thermal maximum and the late-Holocene cooling in the tundra of NE European Russia, *Quaternary Res.*, 75, 501–511, doi:10.1016/j.yqres.2011.01.007, 2011.

Sarnthein, M., Winn, K., and Duplessy, J. C., Fontugne, M. R.: Global variations of surface ocean productivity in low and mid latitudes: influence on CO₂ reservoirs of the deep ocean and atmosphere during the last 21,000 years, *Paleoceanography*, 3, 361–399, 1988.

Schilt, A., Baumgartner, M., Schwander, J., Buiron, D., Capron, E., Chappellaz, J., Loulergue, L., Schüpbach, S., Spahni, R., Fischer, H., and Stocker, T. F.: Atmospheric nitrous oxide during the last 140,000 years, *Earth Planet. Sc. Lett.*, 300, 33–43, doi:10.1016/j.epsl.2010.09.027, 2010.

Shakun, J. D., Clark, P. U., He, F., Marcott, S. A., Mix, A. C., Liu, Z., Otto-Bliesner, B., Schmitner, A., and Bard, E.: Global warming preceded by increasing carbon dioxide concentrations during the last deglaciation, *Nature*, 484, 49–54, doi:10.1038/nature10915, 2012.

Steffensen, J. P., Andersen, K. K., Bigler, M., Clausen, H. B., Dahl-Jensen, D., Fischer, H., Goto-Azuma, K., Hansson, M., Johnsen, S. J., Jouzel, J., Masson-Delmotte, V., Popp, T., Rasmussen, S. O., Rothlisberger, R., Ruth, U., Stauffer, B., Siggaard-Andersen, M. L., Sveinbjornsdottir, A. E., Svensson, A., and White, J. W. C.: High-resolution Greenland ice core data show abrupt climate change happens in few years, *Science*, 321, 680–683, doi:10.1126/science.1157707, 2008.

Stokes, R. C., Tarasov, L., Blomdin, R., Cronin, M. T., Fisher, G. T., Gyllencreutz, R., Hättestrand, C., Hindmarsh, R. C. A., Hughes, L. C. A., Jakobsson, M., Kirchner, N., Livingstone, J. S., Margold, M., Murton, B. J., Noormets, R., Peltier, R. W., Peeteet, M. D., Piper, J. W. D., Preusser, F., Renssen, H., Roberts, H. D., Roche, M. D., Saint-Ange, F., Stroeven, P. A., and Teller, T. J.: On the reconstruction of palaeo-

Effects of melting ice sheets and orbital forcing

Y. Zhang et al.

Title Page

Abstract

Introduction

Conclusions

References

Tables

Figures



Back

Close

Full Screen / Esc

Printer-friendly Version

Interactive Discussion



ice sheets: recent advances and future challenges, *Quaternary Sci. Rev.*, 125, 15–49, doi:10.1016/j.quascirev.2015.07.016, 2015.

Svendsen, J., Alexanderson, H., Astakhov, V., Demidov, I., Dowdeswell, J., Funder, S., Gataullin, V., Henriksen, M., Hjort, C., Houmark-Nielsen, M., Ingolfsson, H. H. O., Jakobsson, M., Kjaer, K., Larsen, E., Lokrantz, H., Lunkka, J., Lysa, A., Mangerud, J., Matouchkov, A., Murray, A., Moller, P., Niessen, F., Nikolskaya, O., Polyak, L., Saaristo, M., Siegert, C., Siegert, M., Spielhagen, R., and Stein, R.: Late Quaternary ice sheet history of northern Eurasia, *Quaternary Sci. Rev.*, 23, 1229–1271, doi:10.1016/j.quascirev.2003.12.008, 2004.

Tarasov, P. E., Müller, S., Zech, M., Andreeva, D., Diekmann, B., and Leipe, C.: Last glacial vegetation reconstructions in the extreme-continental eastern Asia: potentials of pollen and n-alkane biomarker analyses, *Quatern. Int.*, 290–291, 253–263, doi:10.1016/j.quaint.2012.04.007, 2013.

Thornalley, D. J., Elderfield, H., and McCave, I. N.: Holocene oscillations in temperature and salinity of the surface subpolar North Atlantic, *Nature*, 457, 711–714, doi:10.1038/nature07717, 2009.

Thornalley, D. J. R., Elderfield, H., and McCave, I. N.: Reconstructing North Atlantic deglacial surface hydrography and its link to the Atlantic overturning circulation, *Global Planet. Change*, 79, 163–175, doi:10.1016/j.gloplacha.2010.06.003, 2011.

Thornalley, D. J. R., Barker, S., Becker, J., Hall, I. R., and Knorr, G.: Abrupt changes in deep Atlantic circulation during the transition to full glacial conditions, *Paleoceanography*, 28, 253–262, doi:10.1002/palo.20025, 2013.

Vinther, B. M., Clausen, H. B., Johnsen, S. J., Rasmussen, S. O., Andersen, K. K., Buchardt, S. L., Dahl-Jensen, D., Seierstad, I. K., Siggaard-Andersen, M. L., Steffensen, J. P., Svensson, A., Olsen, J., and Heinemeier, J.: A synchronized dating of three Greenland ice cores throughout the Holocene, *J. Geophys. Res.*, 111, D13102, doi:10.1029/2005jd006921, 2006.

Vinther, B. M., Clausen, H. B., Fisher, D. A., Koerner, R. M., Johnsen, S. J., Andersen, K. K., Dahl-Jensen, D., Rasmussen, S. O., Steffensen, J. P., and Svensson, A. M.: Synchronizing ice cores from the Renland and Agassiz ice caps to the Greenland Ice Core Chronology, *J. Geophys. Res.*, 113, D08115, doi:10.1029/2007jd009143, 2008a.

Vinther, B. M., Buchardt, S. L., Clausen, H. B., Dahl-Jensen, D., Johnsen, S. J., Fisher, D. A., Koerner, R. M., Raynaud, D., Lipenkov, V., Andersen, K. K., Blunier, T., Rasmussen, S. O.,

Steffensen, J. P., and Svensson, A. M.: Holocene thinning of the Greenland ice sheet, *Nature*, 461, 385–388, doi:10.1038/nature08355, 2008b.

Wang, Y., Cheng, H., Edwards, R. L., He, Y., Kong, X., An, Z., Wu, J., Kelly, M. J., Dykoski, C., and Li, X.: The Holocene Asian monsoon: links to solar changes and North Atlantic climate, *Science*, 308, 854–857, doi:10.1126/science.1106296, 2005.

Wiersma, A. P., Renssen, H., Goosse, H., and Fichefet, T.: Evaluation of different freshwater forcing scenarios for the 8.2 kaBP event in a coupled climate model, *Clim. Dynam.*, 27, 831–849, doi:10.1007/s00382-006-0166-0, 2006.

Yuan, D., Cheng, H., Edwards, R. L., Dykoski, C. A., Kelly, M. J., Zhang, M., Qing, J., Lin, Y., Wang, Y., Wu, J., Dorale, J. A., An, Z., and Cai, Y.: Timing, duration, and transitions of the last interglacial Asian monsoon, *Science*, 304, 575–578, doi:10.1126/science.1091220, 2004.

CPD

11, 5345–5399, 2015

Effects of melting ice sheets and orbital forcing

Y. Zhang et al.

[Title Page](#)[Abstract](#)[Introduction](#)[Conclusions](#)[References](#)[Tables](#)[Figures](#)[Back](#)[Close](#)[Full Screen / Esc](#)[Printer-friendly Version](#)[Interactive Discussion](#)

Effects of melting ice sheets and orbital forcing

Y. Zhang et al.

Title Page

Abstract

Introduction

Conclusions

References

Tables

Figures



Back

Close

Full Screen / Esc

Printer-friendly Version

Interactive Discussion



Table 1. Boundary conditions for 11.5 ka and pre-industrial (PI).

	11.5 ka			PI*		
Greenhouse gases (GHG)	CO ₂ 253 ppm	CH ₄ 511 ppb	N ₂ O 245 ppb	CO ₂ 280 ppm	CH ₄ 760 ppb	N ₂ O 270 ppb
Orbital parameters (ORB)	ecc 0.019572	obl 24.179°	lon of perih 270.209°	ecc 0.016724	obl 23.446°	lon of perih 102.040°
Ice sheets (relative to present)	Size 69.2 × 10 ⁵ km ²	Max thickness 2331 m	Meltwater flux 220 mSv	–	–	–

PI*: GHG for 1750 AD; ORB for 1950 AD.

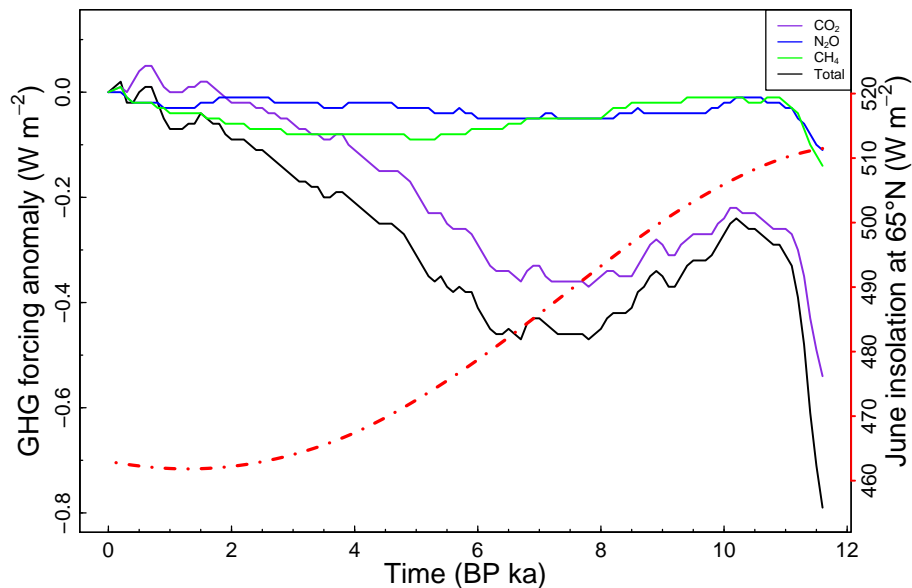


Figure 1. Evolution of greenhouse gas concentration (GHG) shown as the radiative forcing's deviation from the pre-industrial level (with solid lines corresponding to the left axis), and June insolation at 65° N derived from orbital configuration (with red line and the axis on the right).

Effects of melting ice sheets and orbital forcing

Y. Zhang et al.

Title Page

Abstract

Introduction

Conclusions

References

Tables

Figures



Back

Close

Full Screen / Esc

Printer-friendly Version

Interactive Discussion



Effects of melting ice sheets and orbital forcing

Y. Zhang et al.

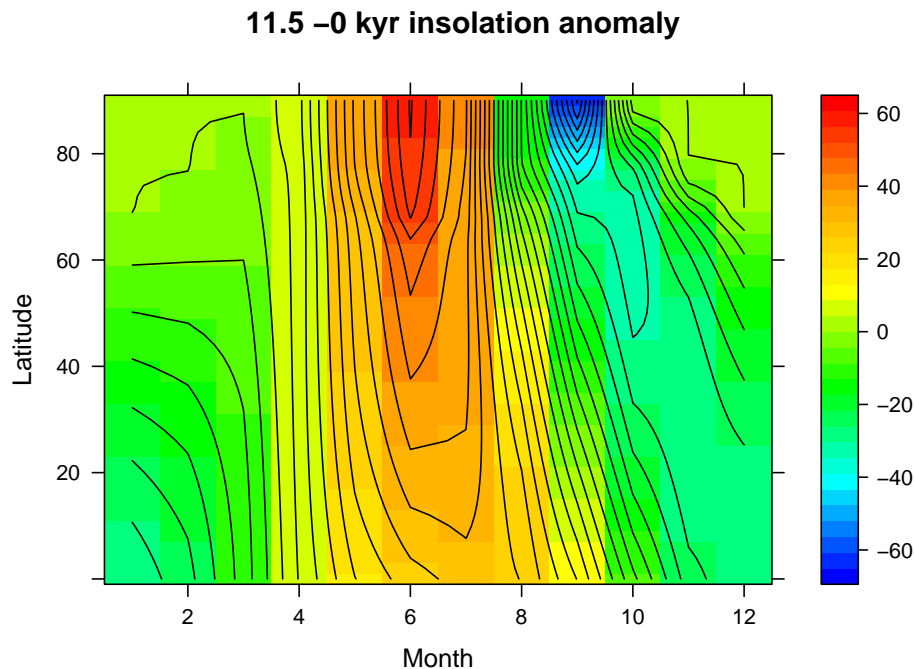


Figure 2. Monthly insolation anomaly (W m^{-2}) at 11.5 ka compared to present derived from Berger (1978).

[Title Page](#)[Abstract](#)[Introduction](#)[Conclusions](#)[References](#)[Tables](#)[Figures](#)[Back](#)[Close](#)[Full Screen / Esc](#)[Printer-friendly Version](#)[Interactive Discussion](#)

Effects of melting ice sheets and orbital forcing

Y. Zhang et al.

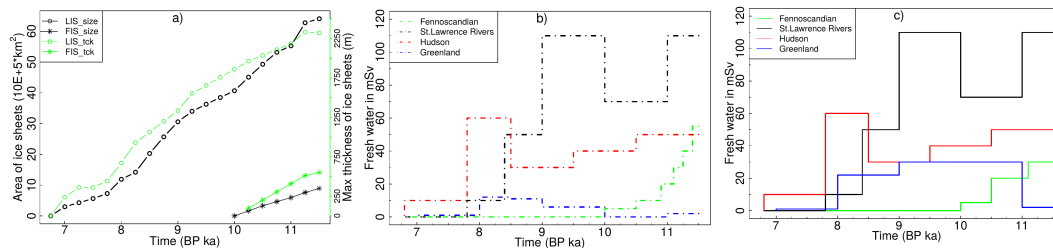


Figure 3. The prescribed ice sheet forcing during the early Holocene. **(a)** Variation of size of ice sheets (km²) displayed as the black lines with the axis on the left and their maximum thickness (m) indicated by the green lines with the axis on the right. A relatively minor change in GIS is not shown due to its small scale; **(b, c)** denote the freshwater flux for the simulation FWF-v1 and FWF-v2 respectively.

Title Page

Abstract

Introduction

Conclusions

References

Tables

Figures



Back

Close

Full Screen / Esc

Printer-friendly Version

Interactive Discussion



Effects of melting ice sheets and orbital forcing

Y. Zhang et al.

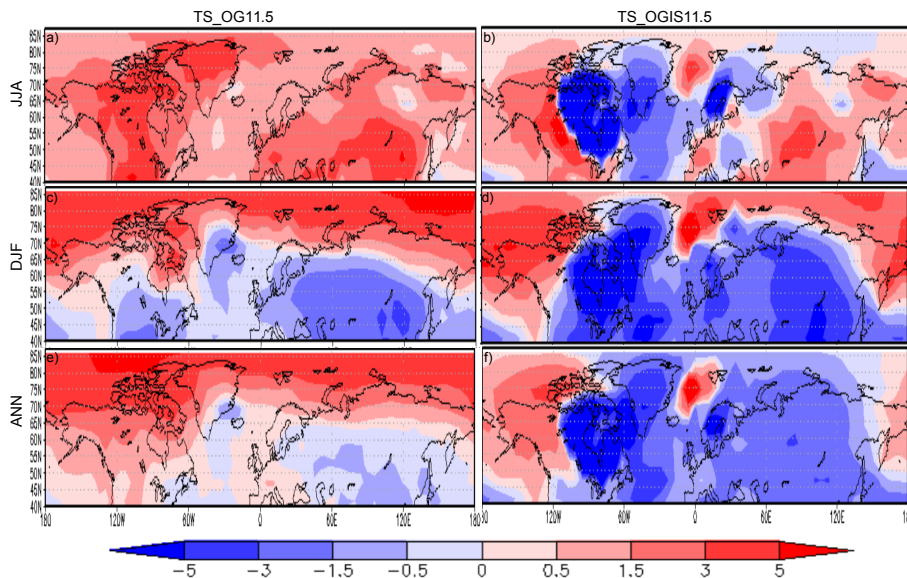


Figure 4. Simulated temperatures for 11.5 ka, shown as deviation from the PI reference. Left column shows the simulation with only GHG and ORB forcing (OG11.5). For the right column, the ice sheet forcing is included (OGIS11.5). Upper, middle and lower panels are summer, winter and annual temperatures respectively.

[Title Page](#)[Abstract](#)[Introduction](#)[Conclusions](#)[References](#)[Tables](#)[Figures](#)[Back](#)[Close](#)[Full Screen / Esc](#)[Printer-friendly Version](#)[Interactive Discussion](#)

Effects of melting ice sheets and orbital forcing

Y. Zhang et al.

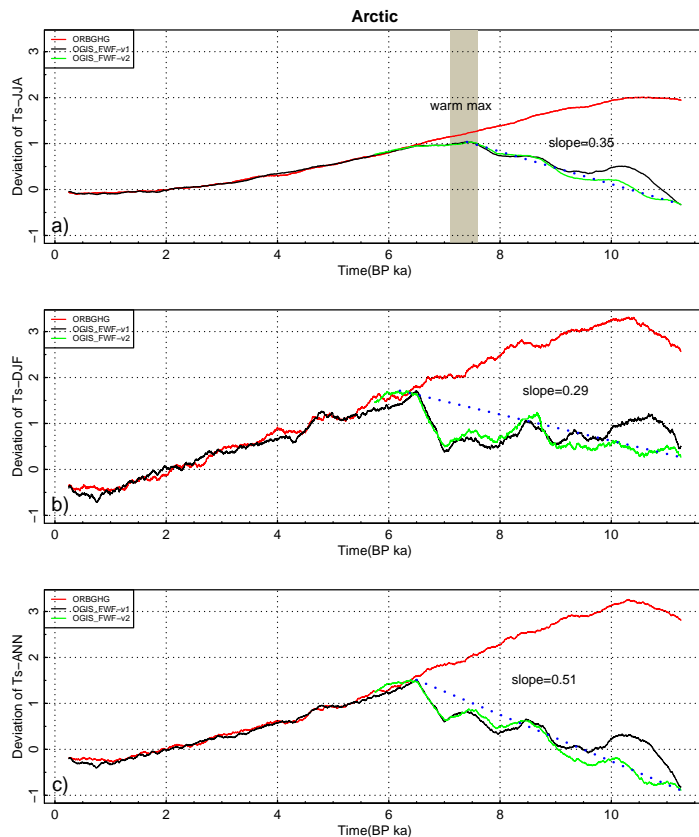


Figure 5. Simulated temperature evolution, shown as the anomalies compared to the PI, since the early Holocene in high latitudes (North of 70°). Red line indicates the simulation with only ORB and GHG forcings (ORBGHG). Black and Green line represent the simulations OGIS_FWF-v1 and OGIS_FWF-v2, in which the ice sheets are included. (a–c) panel represent the summer, winter and annual values respectively.

Title Page

Abstract

Introduction

Conclusions

References

Tables

Figures



Back

Close

Full Screen / Esc

Printer-friendly Version

Interactive Discussion



Effects of melting ice sheets and orbital forcing

Y. Zhang et al.

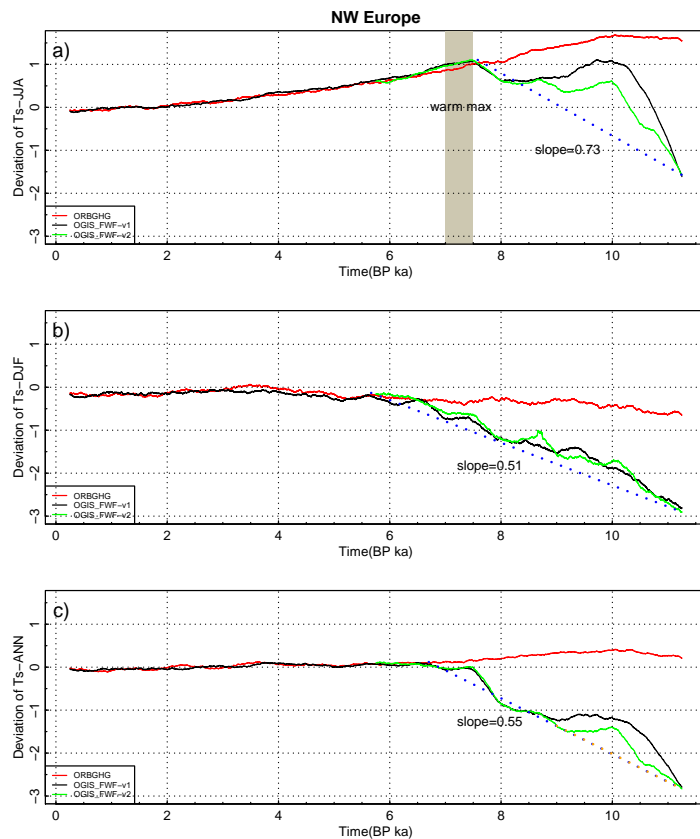


Figure 6. Simulated temperatures, shown as the anomalies compared to the PI, during the Holocene in Northwestern Europe (5° W– 34° E, 58 – 69° N). The caption is same as in Fig. 5.

Title Page

Abstract

Introduction

Conclusions

References

Tables

Figures



Back

Close

Full Screen / Esc

Printer-friendly Version

Interactive Discussion



Effects of melting ice sheets and orbital forcing

Y. Zhang et al.

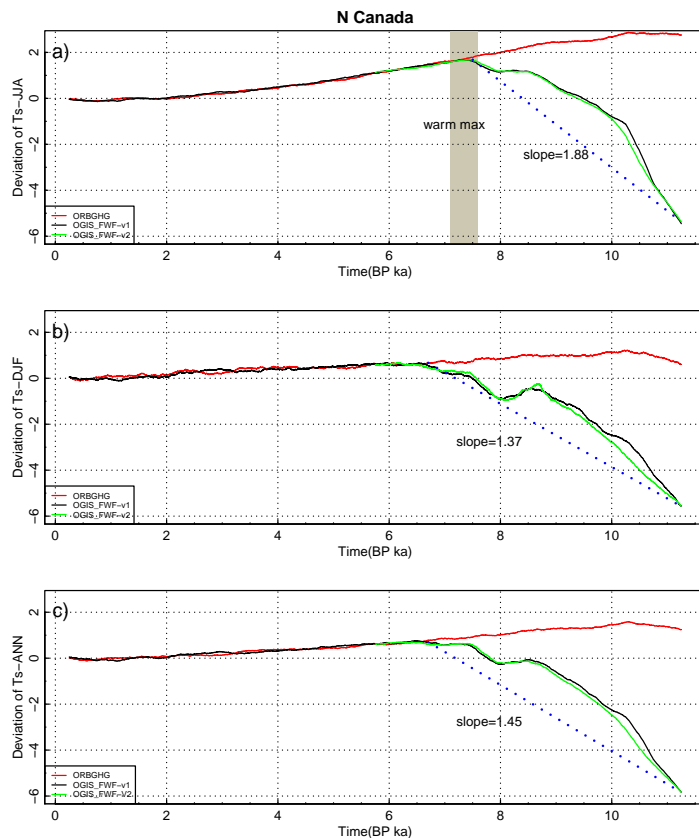


Figure 7. Simulated temperatures, shown as the anomalies compared to the PI, during the Holocene in Northern Canada (120–55° W, 50–69° N). The caption is same as in Fig. 5.

Title Page

Abstract

Introduction

Conclusions

References

Tables

Figures



Back

Close

Full Screen / Esc

Printer-friendly Version

Interactive Discussion



Effects of melting ice sheets and orbital forcing

Y. Zhang et al.

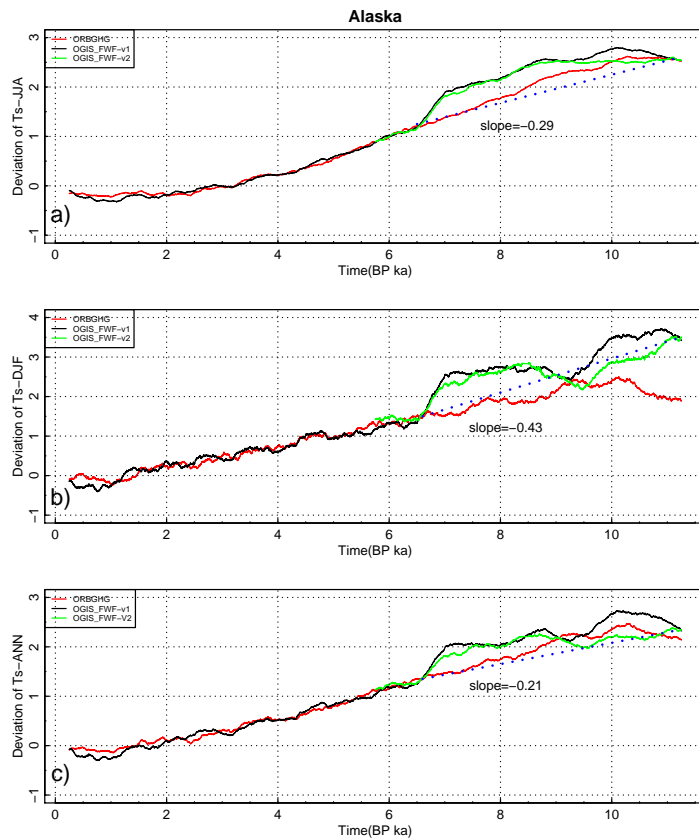


Figure 8. Simulated temperatures, shown as the anomalies compared to the PI, during the Holocene in Alaska (170 – 120° W, 58 – 74° N). The caption is same as in Fig. 5.

Title Page

Abstract

Introduction

Conclusions

References

Tables

Figures



Back

Close

Full Screen / Esc

Printer-friendly Version

Interactive Discussion



Effects of melting ice sheets and orbital forcing

Y. Zhang et al.

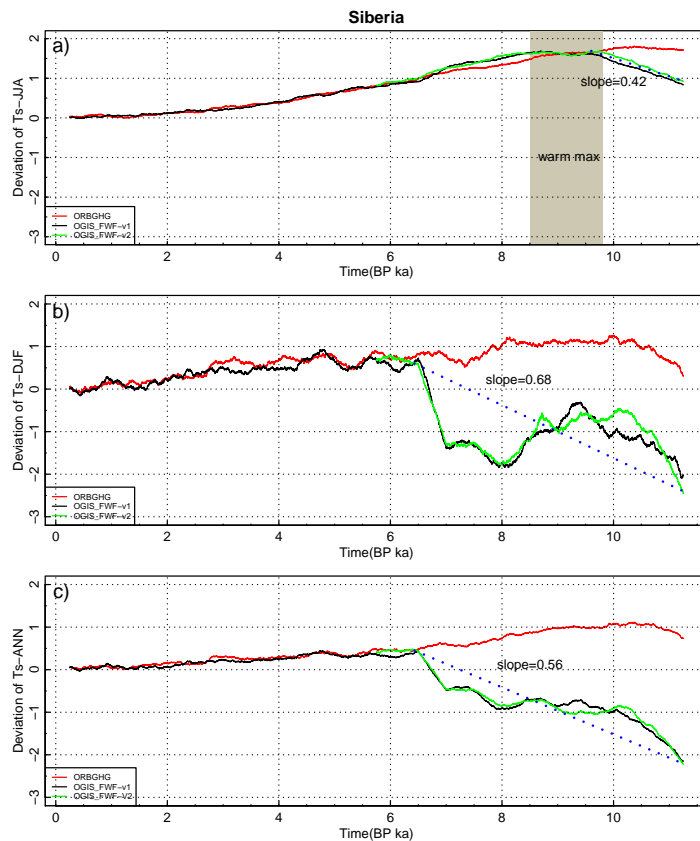


Figure 9. Simulated temperatures, shown as the anomalies compared to the PI, since the early Holocene in Siberia (62–145° E, 58–74° N). The caption is same as in Fig. 5.

Title Page

Abstract

Introduction

Conclusions

References

Tables

Figures



Back

Close

Full Screen / Esc

Printer-friendly Version

Interactive Discussion



Effects of melting ice sheets and orbital forcing

Y. Zhang et al.

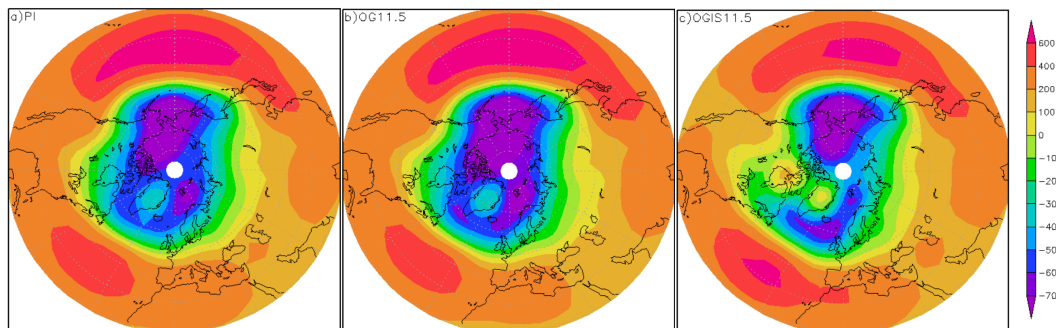


Figure 11. Geopotential height (m) at 800 hPa in the extratropical Northern Hemisphere. **(a)** shows the control condition PI, **(b, c)** are the simulations OG11.5 and OGIS11.5.

[Title Page](#)[Abstract](#)[Introduction](#)[Conclusions](#)[References](#)[Tables](#)[Figures](#)[Back](#)[Close](#)[Full Screen / Esc](#)[Printer-friendly Version](#)[Interactive Discussion](#)

Effects of melting ice sheets and orbital forcing

Y. Zhang et al.

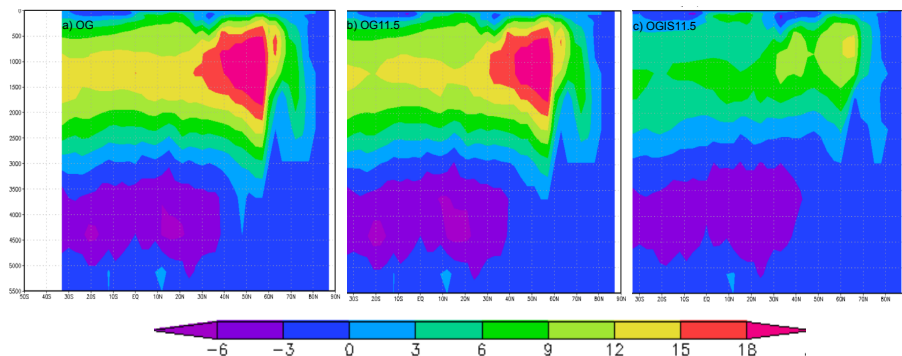


Figure 12. Meridional overturning streamfunction (S_v) in the Atlantic Ocean Basin. (a–c) indicate the control run (PI), the simulation OG11.5 and OGIS11.5 respectively. On the left hand side, depth is indicated in meters. Positive values indicate clockwise circulation.

[Title Page](#)[Abstract](#)[Introduction](#)[Conclusions](#)[References](#)[Tables](#)[Figures](#)[Back](#)[Close](#)[Full Screen / Esc](#)[Printer-friendly Version](#)[Interactive Discussion](#)

Effects of melting ice sheets and orbital forcing

Y. Zhang et al.

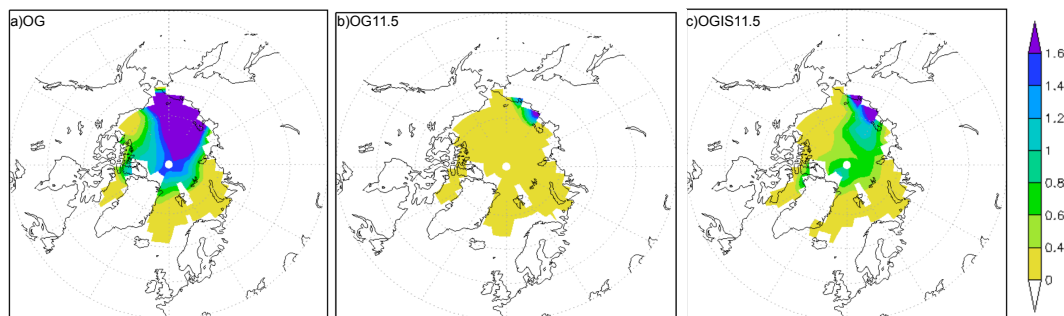


Figure 13. Minimum sea ice thickness (m) in September for PI (a), OG11.5 (b) and OGIS11.5 (c).

[Title Page](#)[Abstract](#)[Introduction](#)[Conclusions](#)[References](#)[Tables](#)[Figures](#)[Back](#)[Close](#)[Full Screen / Esc](#)[Printer-friendly Version](#)[Interactive Discussion](#)

Effects of melting ice sheets and orbital forcing

Y. Zhang et al.

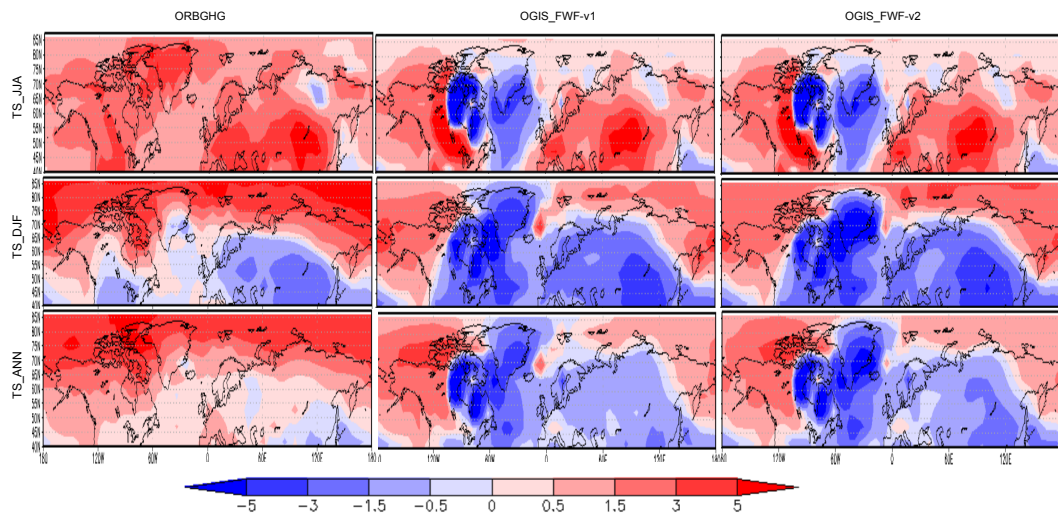


Figure 14. Simulated temperatures for 10 ka (shown as the deviation of 100 yrs average from PI). Left, middle and right columns show the simulation ORBGHG, OGIS_FWF-v1 and OGIS_FWF-v2 respectively. Upper, middle and lower panel indicate summer, winter and annual temperatures.

Title Page

Abstract

Introduction

Conclusions

References

Tables

Figures



Back

Close

Full Screen / Esc

Printer-friendly Version

Interactive Discussion



Effects of melting ice sheets and orbital forcing

Y. Zhang et al.

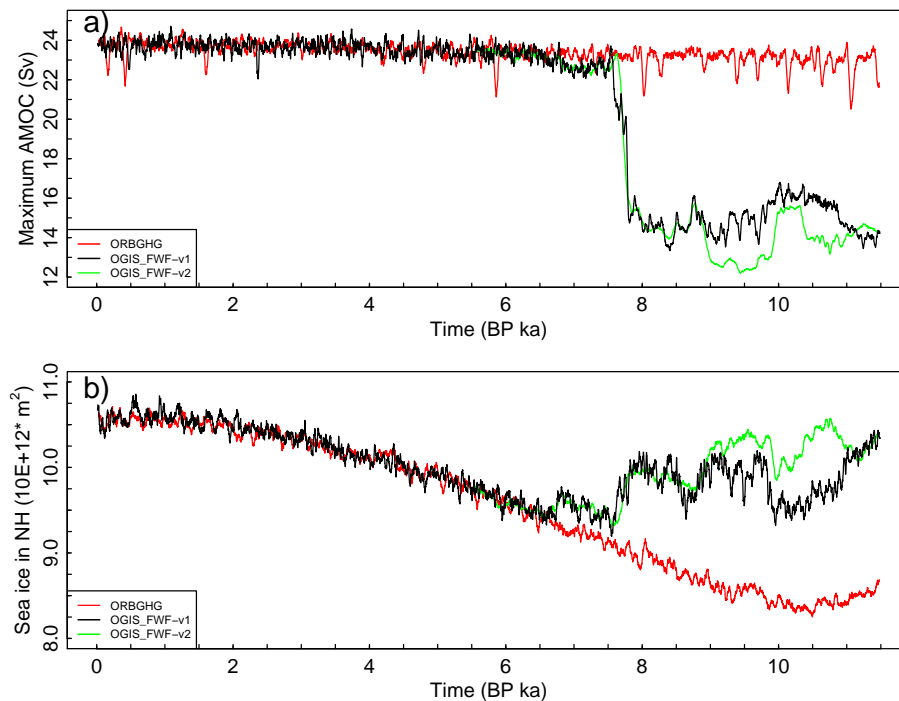


Figure 15. Response of the ocean variables (shown as a 100 yrs average) to forcings during the Holocene. **(a)** Maximum meridional overturning streamfunction (Sv) in the North Atlantic. **(b)** Sea ice area (10^{12} m^2) in the Northern Hemisphere. Red line indicates the ORBGHG simulation. Black and green lines reflect results of the simulation OGIS_FWF-v1 and OGIS_FWF-v2.

Title Page

Abstract

Introduction

Conclusions

References

Tables

Figures

◀

▶

◀

▶

Back

Close

Full Screen / Esc

Printer-friendly Version

Interactive Discussion



Effects of melting ice sheets and orbital forcing

Y. Zhang et al.

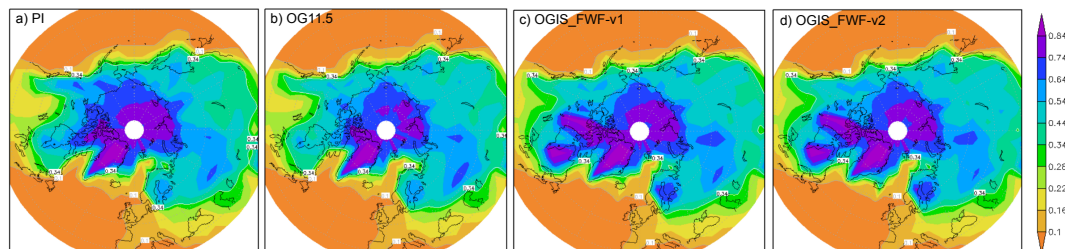


Figure 16. Simulated winter surface albedo shown as a 100 yrs average in the extratropical Northern Hemisphere. **(a)** is for the PI. **(b–d)** represent the simulations ORBGHG, OGIS_FWF-v1 and OGIS_FWF-v2 at 10 ka respectively.

[Title Page](#)[Abstract](#)[Introduction](#)[Conclusions](#)[References](#)[Tables](#)[Figures](#)[Back](#)[Close](#)[Full Screen / Esc](#)[Printer-friendly Version](#)[Interactive Discussion](#)